Implementation of Automatic Inspection System

By

Yugank Chawla

B. Tech Mechanical Engineering

National Institute of Technology, Kurukshetra, 2010

SUBMITTED TO THE DEPARTMENT OF MECHANICAL ENGINEERING IN PARTIAL FULFILLMENT OF THE REQUIREMENTS FOR THE DEGREE OF

MASTER OF ENGINEERING IN MANUFACTURING
AT THE
MASSACHUSETTS INSTITUTE OF TECHNOLOGY

September 2014

Signature redacted

Author:.....
Yugank Chawla
Department of Mechanical Engineering
August 7, 2014

Signature redacted

Certified by:.....
Dr. David E. Hardt
Ralph E. & Eloise F. Cross Professor of Mechanical Engineering, Chairman,
Department Committee on Graduate Students.
Thesis Advisor

Signature redacted

Accepted by:.....
Dr. David E. Hardt
Ralph E. & Eloise F. Cross Professor of Mechanical Engineering, Chairman,
Department Committee on Graduate Students.

This Page intentionally left blank

Implementation of Automatic Inspection System

By

Yugank Chawla

B. Tech Mechanical Engineering

National Institute of Technology, Kurukshetra, 2010

Submitted to the Department of Mechanical Engineering on August 7, 2014

in partial fulfillment of the requirements for the degree of

Masters of Engineering in Manufacturing

Advisor: Dr David E. Hardt

ABSTRACT

Inspection is the formal examination of a product manufactured by any manufacturing process. Inspection process is critical to all the industries as it ensures that a good quality product reach at the end customers. In order to ensure minimum variation in the quality of inspection of a product, industries rely on advanced equipment or gauge to measure the quality parameters of the product. The accuracy of inspection depends a lot on the method and equipments used to inspect a product. However, at AvCarb material solutions, a product called pyrolytic graphite sheet (PGS) is manufactured and at present the types of defects that occur during their manufacturing process can only be identified visually. The problem with using human senses as a tool to perform an inspection is that the accuracy and speed of the inspection vary from person to person based on their experience, their state of mind and other human factors. Automating a visual inspection system ensures minimum variation in the accuracy and speed of an inspection process. This thesis proposes the use of the automatic vision system to perform visual inspection of PGS. The document presents how some software tools can be used to identify and quantify the defects generated on PGS and gives a comparison of the accuracy of identifying a defect through the automatic vision system and accuracy achieved through human inspection.

This Page intentionally left blank

Acknowledgements

First, I would like to express my sincere thanks to my advisor Dr. David. E. Hardt for his guidance which helped making this project a success. I really appreciate his willingness to share his expertise and experience with the group which helped in solving many problems related to the project.

Many thanks to my team mates: Chase Olle and Knute Svenson. Their support and cooperation made this project one of my best experiences of working in teams. It has been a pleasure working with them.

Thanks to Kathryn Rutters and Don Connors, our project supervisors at AvCarb, for sharing their knowledge about the process. They have been very supportive throughout the project. Thank you for assigning us such a great project which was extremely challenging and a great learning experience. Working with AvCarb team has been a wonderful experience.

Thanks to Jennifer Craig, our writing advisor, for her valuable input on writing this thesis. Her suggestions were very helpful in making this thesis a more presentable document.

Thanks to Jose J. Pacheco, Co-director of M.Eng. Program, for managing this program so well and making this an enriching experience.

Finally, special thanks to my parents for being my guiding light through all the tough times of my life and my friends for their constant encouragement. These guys made it possible for me to make it to MIT and survive it.

Table of Contents

List of Tables

List of Figures

Chapter 1. Introduction

This thesis will cover the introduction of an automatic vision system for inspection of the AvCarb heat spreader material. It suggests and specifies the software tools and equipments used to examine different types of defects, and it studies the accuracy achieved in detecting different type of defects through the suggested system.

1.1 Background and Company History

AvCarb Materials Solution was founded in February of 2013 when it was sold by Ballard Power Systems [1]. However, the current factory has existed in some capacity in its Lowell, MA facility since 1964, manufacturing a variety of advanced materials, most notably the heat shields for the Apollo space program. Currently, they specialize in carbon materials, with three main applications: friction applications (*e.g.*, brake pads for automobiles and trucks), electrochemical applications (*e.g.*, gas diffusion layers for fuel cells), and thermal applications (*e.g.*, heat spreaders for the consumer-electronics industry) [2]. The focus of this thesis will be on reducing the lead time of the manufacturing process of the heat spreader material which is used in the consumer-electronics industry.

1.2 Industry Use for Pyrolytic Graphite Sheets

As electronic devices become smaller and thinner, a premium has been placed on the ability of these devices to shed their waste heat in a more efficient manner. As the processing power of electronic devices increases, more waste heat must be removed from the system. For big systems such as desktop computers, the waste heat is removed through conduction through an aluminum or copper heat sink and convection to the air. If the processing power of these systems is increased, the increase in waste heat can be handled by adding a larger fan or heat sink whereas thin electronic devices such as Smartphone, subnotebooks, and netbooks do not have the luxury of space to accommodate a larger fan or heat sink.

Thus, thin electronic devices cannot rely on the usual heat sink and air convection as the prominent means of internal heat transfer. If these devices cannot dissipate their waste heat in an

effective manner, their components can start malfunctioning or melt. Thus, they rely on a class of materials known for its high thermal conductivity, such as pyrolytic graphite sheet that can dissipate heat four times faster than copper [2].

Similarly, this heat spreader material, as it is known at AvCarb, can be used in other industries where heat needs to be moved from the central region through a space with the thickness of the order of tens of microns. The LED light industry relies on this heat spreader material so that they can run the current through their wires and keep the electronics cool for brighter lights [3]. This is important in LED TVs where thinness gives the product an edge in the competition among other players in the industry and excess heat can permanently damage the image on the screen. The fuel cell and battery industries also use heat spreaders in between their fuel cell or battery stacks in order to move heat from the center of their systems to the edges where the waste heat can be removed via a coolant. Using heat spreaders would eliminate the need for an expensive and mechanically complex coolant system running through each of the stack layers [4].

In the commercial space, the driving factor for the need of heat spreaders is the smartphone and TV industries where reduction in thickness is a highly desired characteristic. Thus, as the market grows for smartphones and LED TVs, the market for heat spreaders will grow accordingly. AvCarb is situated very well to potentially capture some of this growing market.

1.3 Motivation

AvCarb recently joined the heat spreader business by using their existing capital assets to learn how to make heat spreader material, which they did successfully. Now, AvCarb is in the process of scaling up their production of the heat spreaders to meet the growing demand of the market as well as adding a new production step to the end of their current production process in order to broaden their customer base. Producing these heat spreader sheets at AvCarb require four key steps: first, the raw sheets of polyimide are interleaved with another material sheet called Graphite foil to create a stack of sheets; second, the stacks are carbonized in a furnace; third, the stacks are graphitized in another furnace, and fourth, the finished heat spreader product

is separated from the Graphite foil sheets, inspected, and packaged for shipping. Lastly, another process that is relevant to this thesis is the calender machine through which AvCarb's customer runs the heat spreader material through in order to achieve the desired uniform thickness. AvCarb is considering adding this process to their production line as part of its initiative to scale up production. More detail of each of these steps can be found in chapter 2.

With the increase in the production rate, there are a number of challenges AvCarb faces. At the heart of these problems is the long lead time the heat spreaders endure due to the time spent in the two furnaces. Furthermore, all of AvCarb's products, not just the heat spreaders, spend time in both furnaces during their production; thus, the heat spreader needs to share time with products from the friction and electrochemical application lines. The most effective way for AvCarb to scale up production is to more efficiently use the time and space they have already set aside for the production of heat spreaders.

To accomplish this, AvCarb needs to cut down the lead time of some or all the steps involved in the manufacturing process of heat spreader material. The focus of this project will be to reduce the lead time of the fourth step of the manufacturing process which is further split into three phases: first, separation of heat spreader material from graphite foil; second, inspection of the final material and third, calendaring of heat spreader material to the final desired thickness. Measures taken to reduce the lead time of each phase are explored in more detail as an individual topic as a thesis for the Masters of Engineering in Manufacturing Program at Massachusetts Institute of Technology. A group of three students worked with AvCarb to apply engineering techniques to reduce the lead time of each step. Chase Olle focused on improving the rate of the separation process of heat spreader material from graphite foil; Knute Svenson focused on setting up and working of calendaring machine; and Yugank Chawla, the author of this document, looked into improving the rate and accuracy of the inspection process of the heat spreader material.

1.4 Background of the inspection process

The yield of the heat spreader manufacturing process at AvCarb is not sufficient, so in order to ensure that the customer receives only the best-quality products, inspection station is

very critical to the manufacturing process of heat spreader material. As AvCarb plans to increase the production rate of heat spreader material, the number of defective sheets will also increase and inspecting more sheets in less time and with high accuracy will become critical to the company. The defects that occur in the heat spreader material are identified visually by humans. (See chapter 3 for details). In order to identify defects in the sheet, the sheet has to be examined at different angles that consumes a lot of time and also there is a variation in accuracy of identifying a defect caused by human factors.

1.5 Problem Statement

As stated earlier, the fourth step of heat spreader manufacturing process is comprised of three phases, out of which the inspection phase of the final material is carried on by workers visually that do not ensure consistency in the accuracy of the inspection process. In both AvCarb's and its customer's visual inspection phase, the workers are looking for nine types of visual defects. These defects fall into two different categories: that caused by the process and that caused by human factors. More information on these defects can be found in chapter 3.

The detection of these defects depends on human judgment, the accuracy of which varies from worker to worker. The inspection of sheet is also a time consuming step as 100 % inspection is needed, and inspection of each sheet takes on average 1 to 2 seconds. The variation in both times taken to inspect a sheet and the accuracy of the inspection process is caused by variation in the experience of different inspectors and also by the difference in difficulty level involved in detecting different types of defects.

The objective of this project is to automate the inspection process with the goal of eliminating the variation in time taken to inspect the sheet and also eliminating the variation in accuracy of the inspection process. This will reduce the lead time involved in the inspection process and will also increase the yield of the process.

1.6 Thesis Overview

Chapter 2 goes into detail of the manufacturing process done at AvCarb, and it gives a better understanding of the physical process used to convert the input material to the finished

heat spreader product, including a description of how the heat of the furnace chemically alters the materials. Also, Chapter 2 will describe the actual manufacturing process done at AvCarb. Chapter 3 gives the details of all the defects occurring on the sheet, their cause of the occurrence and acceptance criteria. Chapter 4 gives the principle behind automatic defect detection and specifications of equipment used for automating the inspection process. Chapter 5 describes how the experimental setup designed for different defects and Chapter 6 shows the results obtained from the experiments and what can be concluded from them. Chapter 7 suggests future work to improve automatic defect detection.

Chapter 2. Manufacturing Process

2.1 Overview

In this chapter, the process of manufacturing the heat spreader is discussed. The first part of this chapter goes into detail of physics underlying the process and how the polyimide material chemically changes into the pyrolytic graphite sheet. The second part of the chapter gives an overview of the actual process done at AvCarb's facility. This chapter will also give an overview of the new process to be introduced at AvCarb in order to reduce the lead time of the final step of the manufacturing process.

2.2 Materials

2.2.1 Polyimide Film

A Polyimide film is the starting material that will be converted to pyrolytic graphite. This film is highly desirable as the precursor for pyrolytic graphite because of its chemical structure and high carbon yield during the carbonization and graphitization process. The molecular structure of the polyimide governs the structure of the final carbonized material [5]. Polyimide films are a high heat resistant material with an amorphous structure dominated by a backbone of hexagonal carbon rings. Organic materials without this in-plane orientation will develop cracks during the heat treatment process. The graphitizability of polyimides largely depends on their in-plane orientation; even a local difference of degree of the orientation induces non-uniform graphitization [18].

2.2.2 Graphite Foil

Graphite foil is flexible graphite made using the powdered form of natural graphite as input material. The powdered form (graphite flakes) is treated chemically with an exfoliating chemical, typically a mixture of hydrochloric acid and an oxidizing agent. The treated powder is exposed to heat, causing the particles to expand. These exfoliated flakes are then mixed with untreated powder and compressed using a roller to form Graphite foil plates. Graphite foil is resilient and compressible, thermally stable, and has a high thermal conductivity [19].

The Graphite foil provides three benefits during the production process. First, the Graphite foil separates individual Polyimide sheets. If two polyimide sheets are in direct contact with each other during the carbonization stage, the surfaces will adhere and become marred; thus, the polyimide sheets must be kept out of contact. Second, the thermal conductivity of polyimide is low ($0.37\frac{W}{mK}$) [20]; therefore, the Graphite foil sheets increase thermal uniformity across the polyimide sheet. Third, the Graphite foil compresses the polyimide, keeping them flat. Without compression, the polyimide will wrinkle and warp during the carbonization phase, which will likely cause the final product to be wrinkled as well.

2.2.3 Pyrolytic graphite sheet

Pyrolytic graphite sheets are thin, lightweight graphite films, which have high thermal conductivity compared to common metals such as copper. Since the material is lightweight, thin, and has a high thermal conductivity, it is used to diffuse waste heat generated in electronic devices such as CPU's, power amplifiers, cameras, and mobile phones. [21]

The useful thermal properties of pyrolytic graphite are the result of its atomic structure. Its carbon rings are oriented in a honeycomb lattice in the same planar direction. The carbon honeycomb is formed of strong bonds between carbon atoms. These high energy bonds dominate the thermal properties of the lattice in the in-plane direction, resulting in very high thermal-conductivity ($\sim 1500\frac{W}{mK}$) [1]. These lattice-planes form layers, which are held together by Van der Waals interactions. These Van der Waals interactions between layers are comparably weaker, which results in a much lower thermal-conductivity ($\sim 10\frac{W}{mK}$) in the cross plane direction.

2.3 Physical Process

The physics of making the heat spreader is a two-step process: carbonization and graphitization. In this section, the carbonization and graphitization steps of one type of polyimide film are explained. Different type polyimide films can react to these processes differently based on their chemical composition.

2.3.1 Carbonization of Polyimide Film

Carbon films are obtained by carbonization of polyimide up to 1000 °C in between Graphite foil plates [6]. Graphite foil plates have high thermal conductivity in the in-plane direction, which helps distribute the heat evenly across the polyimide sheet while in the furnace.

Also, the Graphite foil plates add weight on top of the polyimide sheets and ensure that the sheets are under compression, which prevents them from folding and wrinkling during carbonization (see Figure 1).

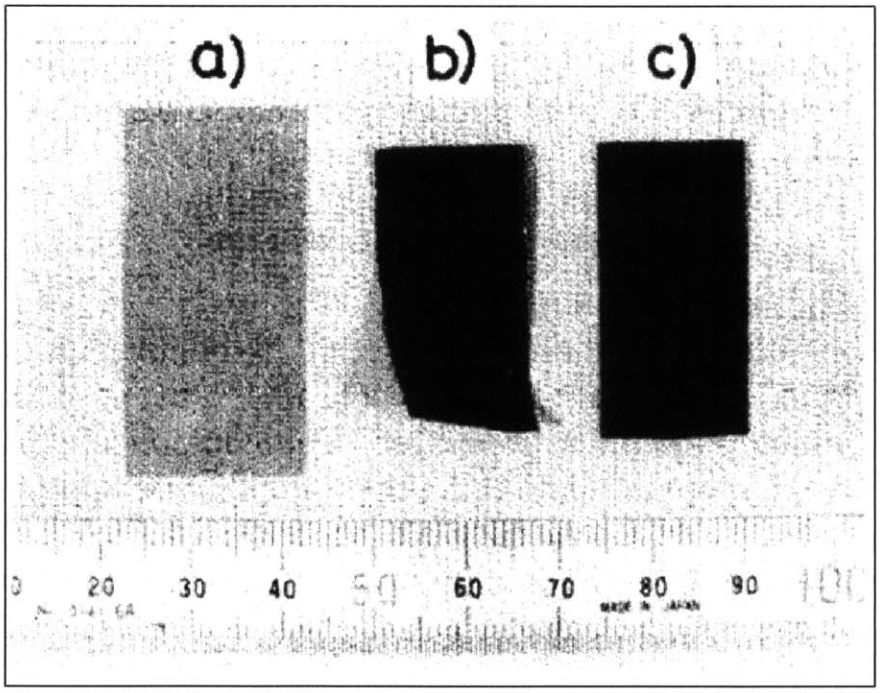

Figure 1: Effect of compression on the appearance of polyimide film (a) original (b) after carbonization at 800 °C without any compression, and (c) after carbonization at 800 °C under compression of plates [6]

During the carbonization process, the polyimide used undergoes pyrolysis that removes the majority of the non-carbon elements of the material. The sheets are raised to a temperature of 500 °C – 650 °C, which results in the breakdown of the carbonyl groups of the polyimide [5]. Carbonyl functional groups are represented by a carbon atom double-bonded to an oxygen atom.

As the bonds of these groups are broken, oxygen is ejected in the form of CO and CO_2. During this step, the polyimide loses about 30% of its weight and shrinks. In the second step where hydrogen and nitrogen gases are released, the temperature is raised above 700 °C. Here, the weight decreases by an additional 10%, and the electrical conductivity increases by an order of magnitude [5]. The hydrogen atoms are typically ejected as either H_2 or CH_4. The nitrogen atoms are released exclusively as N_2 gas.

Figure 2 demonstrates the type and amount of the ejected gases with respect to the temperature of the material in the furnace. Figure 3 shows the amount of oxygen and nitrogen left in the material over a temperature range.

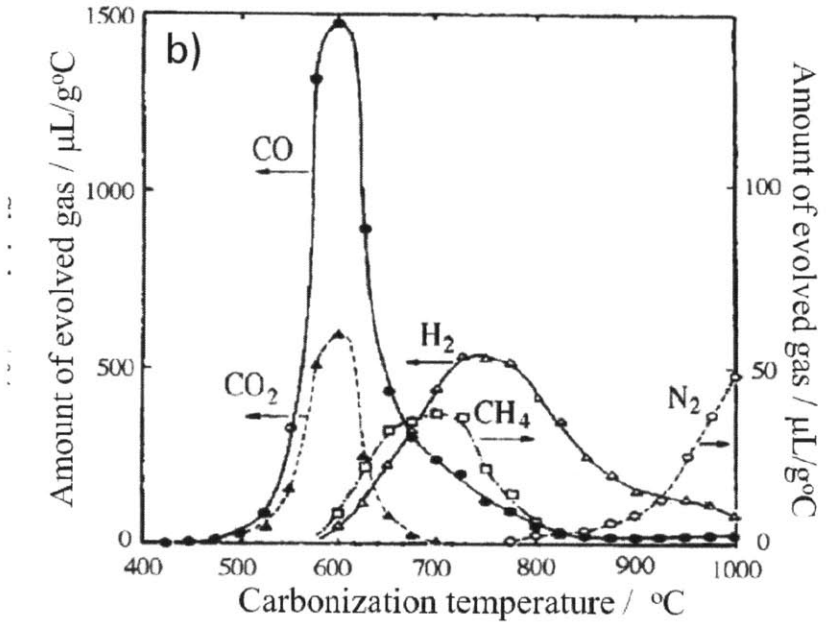

Figure 2: Figure showing amount of evolved gases vs carbonization temperature [5]

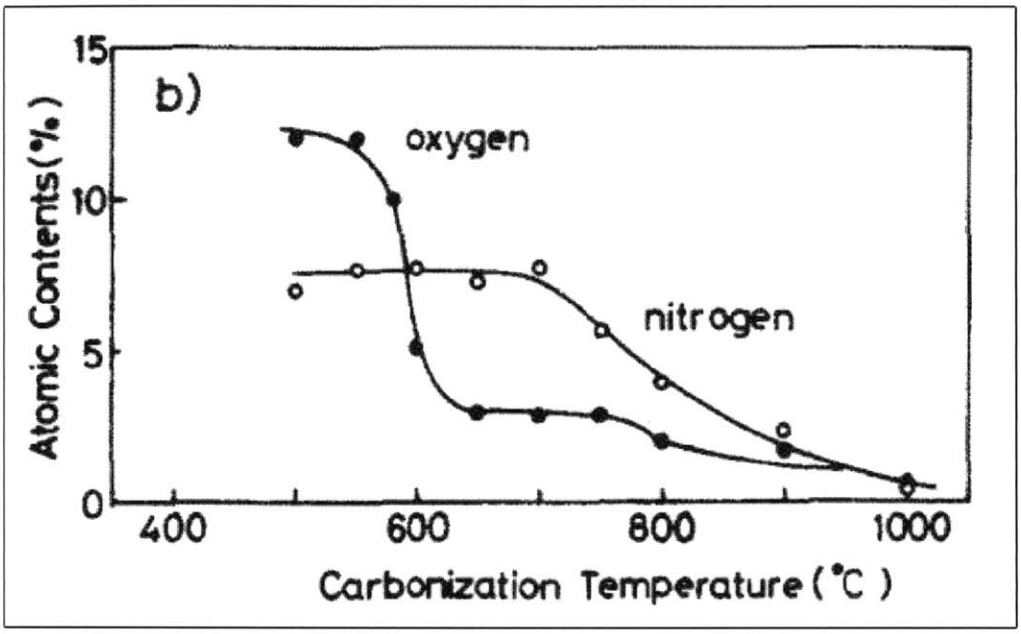

Figure 3: Changes of oxygen and nitrogen contents with carbonization temperatures [6].

The carbonized material retains a granular, glass-like carbon structure and is shiny and fairly rigid [7]. The carbonized sheets are found to weigh 40% less than original polyimide used and decrease in area by as much as 23% after carbonization (See Fig 6). The material also undergoes an increase in electrical conductivity of $65 \frac{S}{cm}$ [6]. The increase in electrical conductivity can be attributed to the development of hexagonal carbon layers formed in the carbonization step. Figure 4 shows the weight loss and decrease in size of the polyimide with respect to changes in temperature of carbonization.

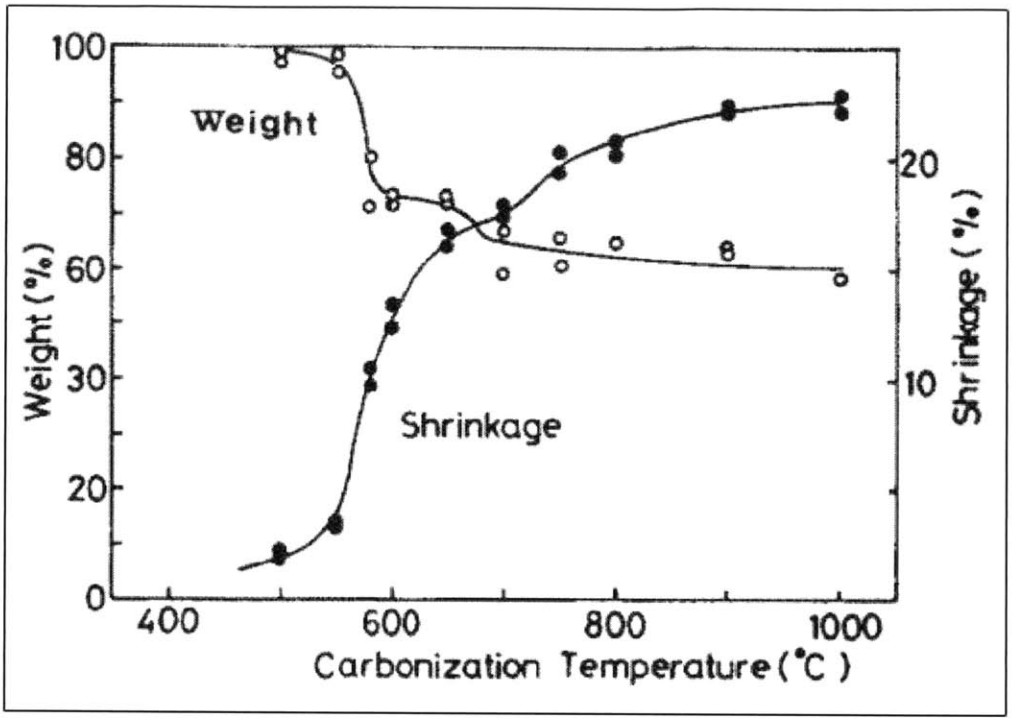

Figure 4: Changes in weight and size at various carbonization temperature [6].

2.3.2 Graphitization of Polyimide Film

After carbonization, the sheets are heat treated up to temperatures of 3100 °C – 3200 °C under atmospheric pressure in an environment of inert gas such as argon [8].

The heat treatment rearranges the molecules of the carbonized sheets into highly-crystalline and highly-oriented structures by inducing a change in the bonding pattern of the carbon. The resultant graphite films have high thermal and electrical conduction properties due to this crystalline structure. A representation of the molecular structure of graphite films is shown in Figure 5.

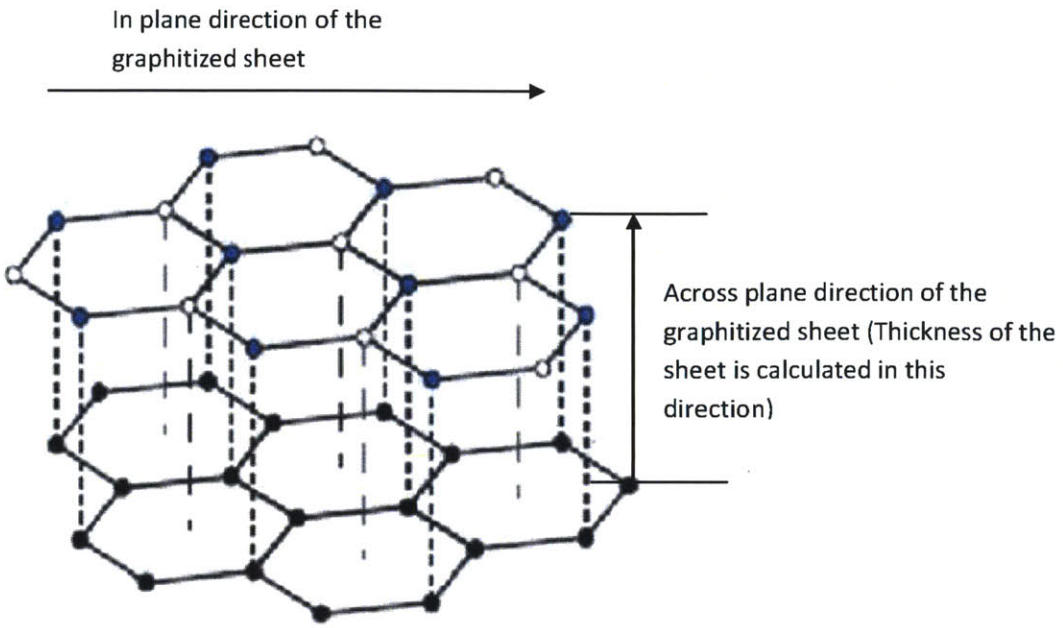

Figure 5: Representation of the molecular structure of Graphitized sheets [9].

The thickness of the carbonized sheet can decrease by 50%. However, the length and width of the sheet can increase by 9-18%. This increase in size is caused by the carbon bonds becoming graphitized and the wrinkles on the carbonized sheet flattening out [10].

2.4 Process at AvCarb

This section will describe the manufacturing process of turning a polyimide sheet into pyrolytic graphite sheets (or heat spreaders) at AvCarb.

Figure 6 shows the transformation of the polyimide sheet used at the AvCarb to the heat spreader material through the carbonization and graphitization process and the corresponding changes in size. The process at AvCarb goes through four key processes: stacking, carbonization, graphitization, and unstacking/inspection (See Figure 7).

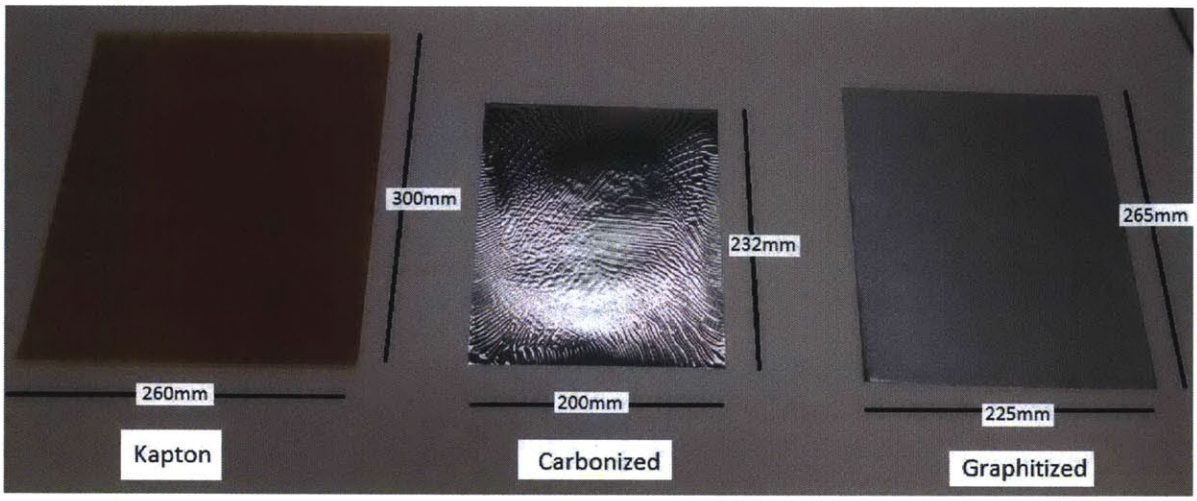

Figure 6: A pictorial progress of the raw material (Kapton) turning into its final graphitized product

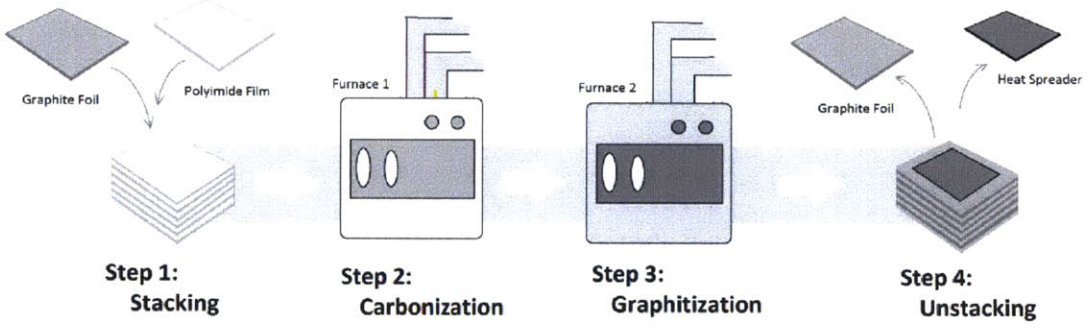

Figure 7: Figure showing the process flow of heat spreader manufacturing at AvCarb

2.4.1 Stacking

In the stacking process, workers will manually interlayer the polyimide and Graphite foil sheets.

2.4.2 Carbonization

The first heat treatment process at AvCarb occurs in a large carbonization furnace, an electric furnace where the material is heated to key temperatures to boil off gases, such as

oxygen and nitrogen. This process occurs under vacuum; therefore, prior to heating the furnace must be checked for any leaks, which typically takes a few hours. The heating process occurs and carbonization of polyimide film takes place.

Next, the furnace is turned off, and the material is allowed to cool to room temperature. A vacuum pump is used during the process to evacuate any toxic gases, such as hydrogen cyanide (HCN) that are formed during the production process.

2.4.3 Graphitization

In the second heat treatment process, the stacks are placed in the graphitization furnace. Here, the material is heated to the required temperature and held at temperature for a period. Unlike the previous furnace, which kept the contents under vacuum, this induction coil furnace maintains an environment of inert gas. The process begins under a nitrogen gas environment and switches to argon at around 1000 °C. After the hold, the furnace is shut off, and the material is cooled to room temperature.

2.4.4 Unstacking and Inspection

Finally, the material is moved out of the induction coil furnace and into the unstacking room, where workers manually separate the finished product (the heat spreader) from the Graphite foil.

The workers will manually inspect both sides of the finished product looking for various kinds of defects, such as wrinkles, spots, unconverted material, and chromic aberration (See chapter 3 for details of defects). Any product that passes the inspection phase is placed in a box for good material, and any product that is rejected for any reason is placed in a manila folder (and the reason for rejection is marked down).

Then after one stack is unstacked, the worker will measure the thickness of four products (equally spaced from top to bottom) from the folder of good material to ensure the material meets its thickness specification. Each Graphite foil sheet can be used multiple times before replacement.

Finally, the finished product is wrapped in its box, vacuum-sealed, and shipped to AvCarb's customer. Their customer will do the sampling inspection of the material received .From these results, the customer will either accept or reject the whole batch of materials; thus, it is very important that AvCarb has a quality inspection process. If the material passes through their customer's inspection process, the customer calenders the material to a uniform thickness and places it on a polyester sheet for easier handling. It is at this stage that the final product achieves its high thermal conductivity and is named pyrolytic graphite sheet. This material then moves down the supply chain where it is die cut into the required shapes and sold to consumer electronics manufacturers who assemble the pyrolytic graphite sheets into their products.

2.5 New process overview

In order to reduce the lead times involved in the manufacturing process of the heat spreader material, a new process is developed for the processing of sheets after graphitization step.

The new process introduces four new steps (See Figure 8). In the first step, a vision system inspects the material leaving the unstacking process. By using a computer vision system the process can eliminate the need for manual inspection. This will reduce the burden on the operators and reduce the variance in acceptance rates. This thesis is primarily concerned with this step of the process.

In the next step, a robotic manipulator will place sheets of heat spreader material onto a polyester film. The tolerance and repeatability requirements for placement are very high. Therefore, it would not be feasible to have an operator manually place sheets. This step is covered in Chase Olle's thesis [23].

After the sheets have been placed on the polyester film, the film passes through a calendering machine. This step turns the process from a discrete batch process into a semi-continuous process. The calendering process gives the heat spreader material several beneficial properties. This step is covered in Knute Svenseon's thesis [24].

Last, the entire film line is rewound into a roll. The finished product is now ready for shipment.

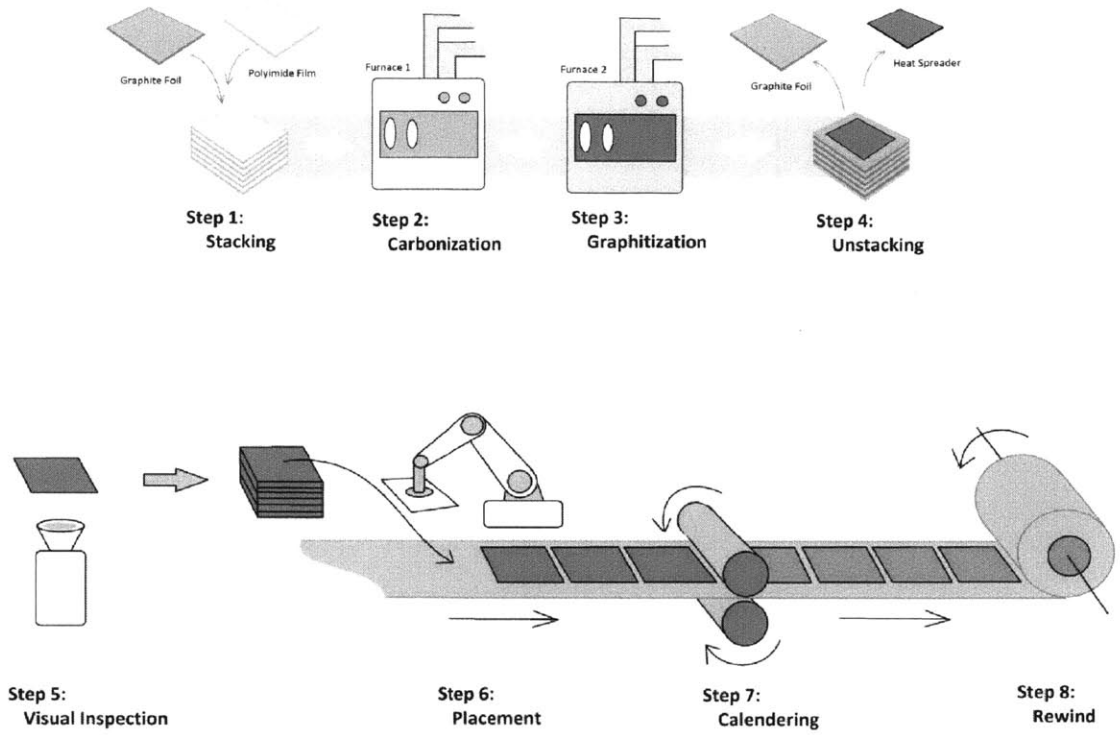

Figure 8: The new production process with four additional steps [23].

Chapter 3. Understanding the defects

3.1 Overview

In this chapter, different types of surface deformities on heat spreader material and its acceptance criteria are explained. This chapter also explains the current methodology to differentiate minor deformity from a deformity that can be categorized as a defect and explains reasons for occurrence of different types of defects.

3.2 Different types of defects

Since the start of production of heat spreader material, several defects have occurred and still generally occur and these defects are broadly divided into nine categories based on their appearance.

3.2.1 Ripples

Identification: This defect has a wave like pattern having crests and troughs of varying heights (see Figure 9).

Reason: These defects are caused by wrinkles that form during the carbonization step. In certain cases, these ripples can persist through the graphitization step. The ripples also denote areas of unconverted material, which is highly undesirable.

Acceptance criteria: The wave pattern that has a crest or a trough height greater than 12.5 microns from the surface of sheet or showing a color difference (more shiny) from the rest of the sheet is categorized as a defect and the sheet having this defect is rejected [17].

Identification methodology: Ripples having a visual color difference from the rest of the sheet are rejected irrespective of the crest or trough height. Ripples that do not have a color difference from the rest of the sheet are identified visually and are first segregated based on human judgment, and then those sheets are checked for the height of crest and trough.

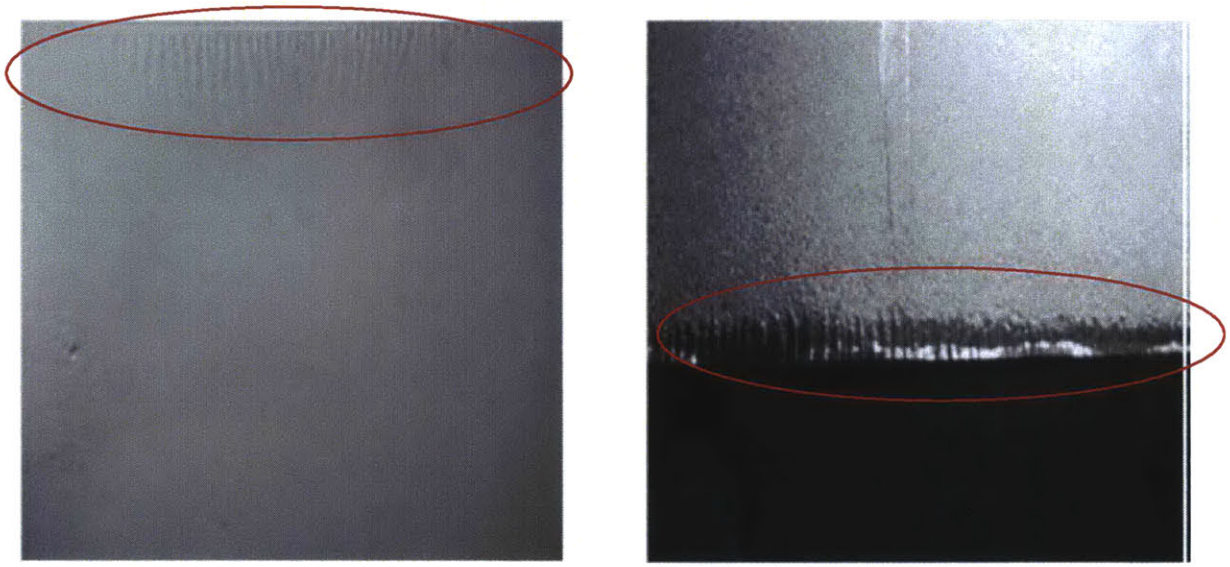

Figure 9: Figure showing ripples on the left image (encircled) and unconverted sheet on the right image (encircled).

3.2.2 Holes

Identification: When a sheet is placed in front of a light source and the light passes through the sheet, then that sheet is classified as a sheet having holes (See Figure 10) [17].

Reason: The occurrence of this defect is caused by miss handling of the product or by the non uniform stresses developed in the sheet while in the processing phase.

Acceptance criteria: If there is even a single visible hole in a sheet irrespective of its shape and size, the sheet is rejected [17].

Identification methodology: This defect is identified visually by facing the sheet in front of a light source.

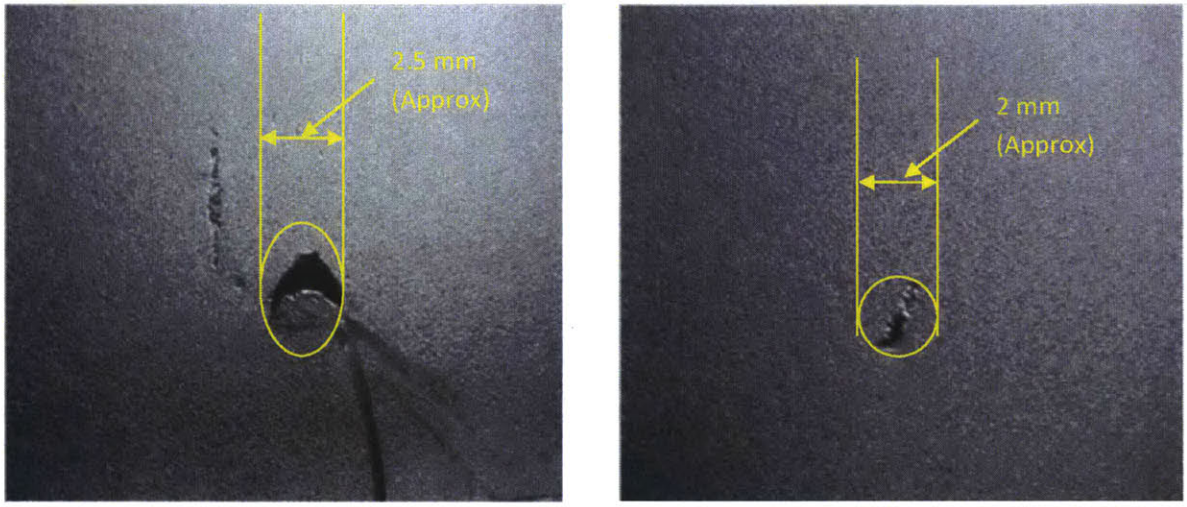

Figure 10: Figure showing two samples of sheet having holes in the marked area.

3.2.3 Dents

Identification: These defects can be identified as an uneven area covering some part of the sheet (see Figure 11).

Reason: In some sheets, carbon residuals from the surroundings of the sheet during processing settle down on the surface of the sheet. These tiny particles are removable but if left behind leave a surface deformity on the sheet.

Acceptance criteria: A dent having a height greater than 13 microns when measured from the surface of the sheet can be categorized as a defect and a sheet having even a single such defect is rejected [17].

Identification methodology: These defects are checked visually, and the doubtful cases are measured using calipers.

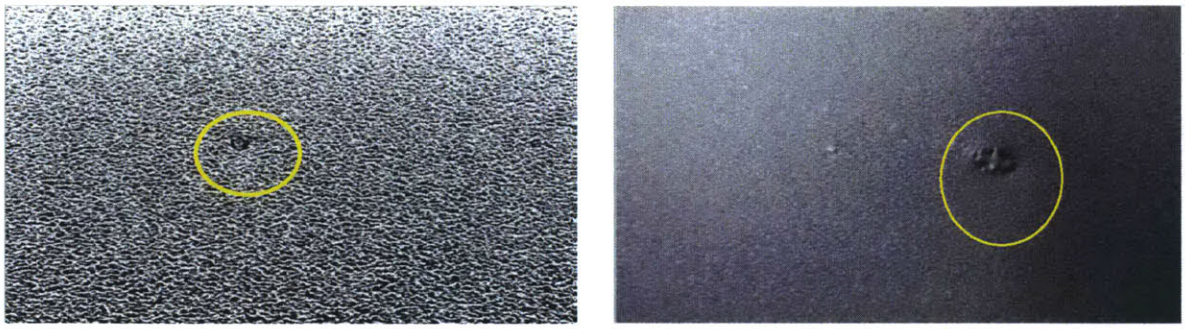

Figure 11: Figure showing sheets having dents in the marked area

3.2.4 Spots

Identification: These defects are identified as shiny small circular areas on the surface of the sheet (Figure 12).

Reason: Possible reason for this type of defect is moisture remaining on the surface of the sheet at the start of its process leading to improper conversion of carbonized sheet to graphitized sheet in tiny areas.

Acceptance criteria: Sheets having spots with the diameter greater than 3mm or having four or more spots having a diameter between 1mm and 3mm are rejected. Sheets having spots less than 1mm is accepted regardless of the number of such spots [17].

Identification methodology: Sheets having spots are segregated visually and their diameter is measured.

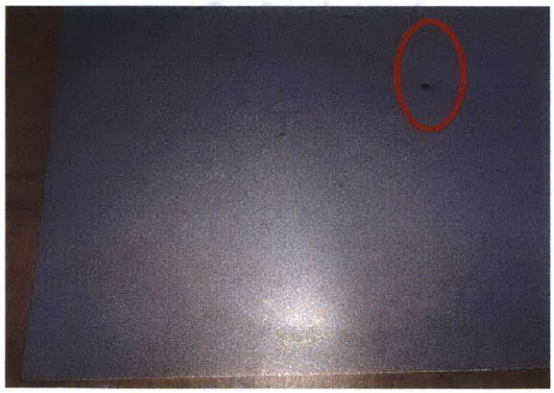

Figure 12: Figure showing spot in the marked area

3.2.5 Chromic aberration

Identification: A large area of sheets having a color different from the rest of the sheet (surface shinier than the rest of the surface) is identified as chromic aberration. The shiny area is always higher in thickness as compared to the rest of the sheet and visually the surface texture of the shiny area is different from the rest of the sheet (Figure 13).

Reason: The possible cause of occurrence of this defect is that heat is not properly spread over the Polyimide material while processing leading to improper conversion of carbonized sheet to graphitized sheet. Experiments have been conducted where different types of graphite foils were used in the process of making heat spreader material, and it has been observed that the presence of chromic aberration depends on the quality of graphite but still the root cause for the occurrence of the defect has not been identified yet.

Acceptance criteria: Chromic aberration is measured based on its detection ability, which solely depends on human judgment. The sheet in which the area is easily identifiable without observing it from different angles is categorized as sheet having high chromic aberration and is rejected where as the sheet in which the affected area is not very easily identifiable and is more evenly spread over the surface is categorized as a sheet with low chromic aberration. The acceptance criteria are very subjective for this defect.

Identification Methodology: The surface of the sheets is inspected visually.

Figure 13: Figure showing chromic aberration in the marked area

3.2.6 Scratch

Identification: These defects look like rubbing marks or line marks on the surface. (Figure14).

Reason: The scratch on the surface occurs because of rubbing of surface against any object.

Acceptance criteria: Sheets having deep scratches are not accepted. The depth/ severity of scratch is also subjective, and no measurable criterion exists to identify the acceptable and non acceptable scratch [17] (Figure 14).

Identification Methodology: This defect is detected visually.

Figure 14: a) Image on left have scratches that are unacceptable b) Image on the right has scratch that is acceptable

3.2.7 Cracks

Identification: These are identified as torn out regions of the sheet (Figure 15).

Reason: The cause of this defect is improper handling.

Acceptance Criteria: Any sheet having even a single crack or missing area is rejected [17].

Identification Methodology: These defects are inspected visually.

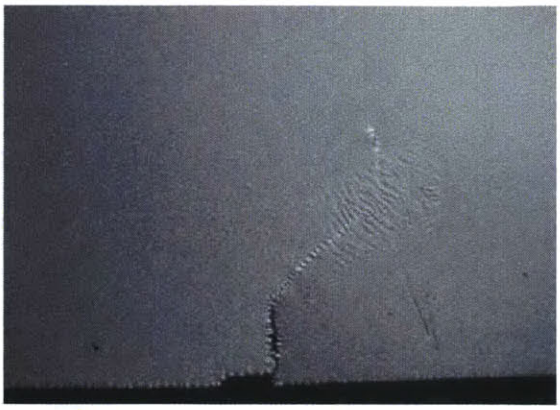

Figure 15: Figure showing crack on the sheet

3.2.8 Distorted edges

Identification: The edges are not straight in a sheet. It is either broken or have a non uniform shape (See figure 16).

Reason: The reason for this defect is the development of non uniform stresses in a sheet while processing.

Acceptance criteria: Any sheet having deformed edges is rejected [17].

Identification Methodology: This defect is identified visually.

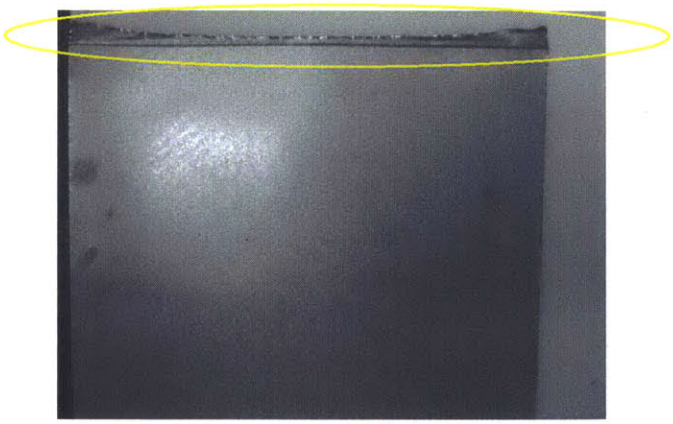

Figure 16: Figure showing deformed edge in the marked area

3.2.9 Angled Edges

Identification: A sheet having an edge that is not perpendicular to its adjacent edge is identified as a defective sheet (See Figure 17).

Reason: The reason for this defect is the development of non uniform stresses in a sheet while processing.

Acceptance criteria: A sheet having an edge with one of its corners offset from another corner by 3mm or more is rejected (See Figure 17). [17]

Identification Methodology: This defect is identified by using calipers.

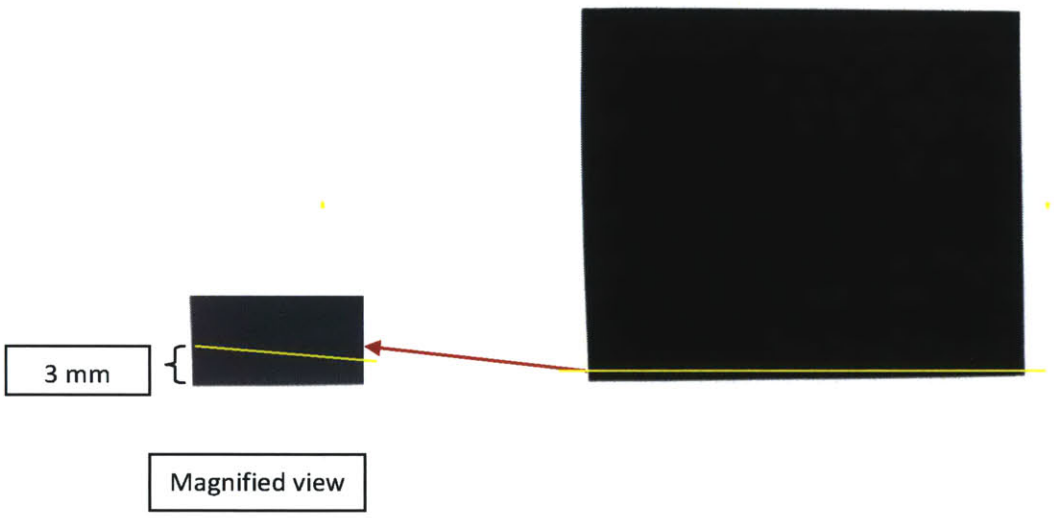

Figure 17: Figure Showing Angled edge defect

Chapter 4. Automatic defect detection

4.1 Overview

This chapter explains the approach taken to automate the inspection process, the basic principle behind the automatic defect detection system chosen for this application, the specifications of the equipments used to automate the process and the setup of the experiments done to identify all the defects.

4.2 Approach

In order to automate the inspection process, automatic quality inspection systems of various industries were studied, particularly the ones used in metal printing industry. The inspection processes of metal printing industries were chosen to study because the quality of their product is defined by the quality of print on the surface of the metal which could not be specified without using a visual inspection system, and the same is the case with detecting defects in heat spreader material. Since several metal printing industries are successfully using the automatic vision system to determine the quality of their product, the same was chosen to automate the inspection process for the heat spreader material.

4.3 Principle of Automatic vision system

In order to automate the inspection process of the heat spreader material, digital images of the material are taken and analyzed for defects using image processing techniques.

4.3.1 Image processing

When a computer receives and uses an image as the input signal, it is called digital image processing [11]. The input signals can be manipulated using computer algorithms to extract meaningful information from an image.

Digital image analysis through image segmentation is used in various applications like

- Feature extraction
- Pattern recognition

- Feature comparison
- Edge detection

All these applications are useful in detecting defects in the heat spreader material.

4.3.2 Image segmentation

Image Segmentation is the process in which an image is divided into parts. In this step, objects or other entities of interest are extracted from an image for analysis. [12].

Image segmentation is based on the principle that the pixels of an image in a specific region are similar in some characteristics such as color, intensity or texture [13]. Image segmentation techniques are used to divide the different regions in an image based on similarity of characteristics of the pixels in that region.

4.4 Equipment Used

The equipment used for automating the inspection process can be categorized into three parts.

4.4.1 Camera

A camera is used to capture the image and send it to the computer in the form of digital signals.

Key considerations for selecting the camera

1. The resolution of the camera has to be sufficient to detect the smallest possible defect in size that can occur in the material (1mm in our case) without detecting any finer details in an image which creates noise.
2. The camera should be able to detect lights of different wavelengths, so that defects can be observed under different lighting conditions.
3. The camera should be able to detect and process an image in less than 10 Sec as it is the target cycle time for the inspection process.

For this project, the camera used to detect the image of heat spreader material is a "Baumer VC XC100M12X00EP" (See figure 18) and its specifications are listed in Table 1. This camera was chosen as it was fulfilling all the key considerations listed for selecting the camera. As can be observed from Table 1, the camera is capable of detecting a surface deformity of size

less than 1mm (High image resolution), detecting light of wavelength beyond visible range and was able to process an image in less than 10 Sec.

Note: Any camera fulfilling the key considerations set for it to conduct the experiments can be used, The decision to choose "Baumer VC XC100M12X00EP" was also based on reviews of its performance in other industries using it for similar applications.

Table 1: Table giving the specifications of the camera used [14]

Feature	Specification
Resolution	1280X960 pixels
Minimum Object distance [Lens used: Visumatix VS0814-H1 (focal length 8mm)]	100 mm
Sensor (monochrome)	1/3" CCD
Speed (High resolution mode)	Max. 12 Insp. /Sec
Defect image memory	8
Features per job	32
Type of light that can be detected	Visible and infrared

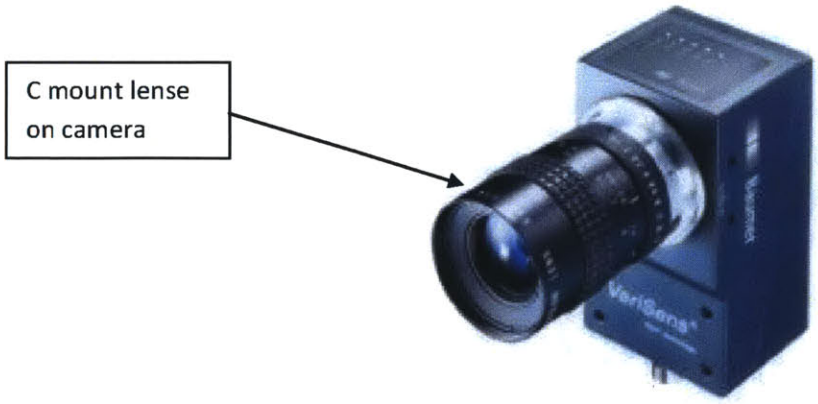

Figure 18: Figure showing the camera used for detecting the defects (Baumer VC XC100M12X00EP)

4.4.2 Lighting

Key considerations for selecting the light

1. The lighting should be uniform, intense and be able to be diffused by the surface of heat spreader material.
2. There should be even illumination.
3. Not susceptible to hindrance caused by ambient light. For example Infrared lights or Ultraviolet lights.

The following lighting is used:

Backlight: Infrared Backlight illumination is used to create maximum contrast between the object and its surroundings which makes detecting object boundaries very easy. The area backlight being used is "Metaphase MB-BL10X12-IR-24". Its specifications are listed in table 2.

Table 2: Table showing specification of backlight used [15]

Feature	Specification
Power Source	24VDC
Current Draw (max)	2.2 ~ 3.0 amps
Cable	10 foot / (3.05 m) cable with flying leads
Housing	Aluminum
Operating Conditions	-30 °C to 60 °C
Lifetime Expectancy	75,000 hours
LED color	Infrared (wavelength: 880nm)

The "Metaphase MB-BL10X12-IR-24" was chosen as it was having an area of 10 inches X 12 inches (See figure 19), which was ideal to contain the final product under inspection as its

dimensions are approximately 10 inches X 8 inches (See figure 6 for dimensions of final product).

Figure 19: Figure showing backlight used ("Metaphase MB-BL10X12-IR-24")

Linear Illuminator: Infrared LED linear illuminators are used to provide uniform lighting over the sheet. The linear illuminator used is "Metaphase ISO-8-IR-24" (See figure 20). Its specifications are listed in table 3.

Table 3: Table showing the specifications of linear illuminators used [16]

Feature	Specification
Power Source	24VDC
Current Draw (max)	0.4 amps
Cable	10 foot / (3.05 m) cable with flying leads
Housing	Aluminum
Operating Conditions	-30 °C to 60 °C
Lifetime Expectancy	75,000 hours
LED color	Infrared (wavelength: 850nm)

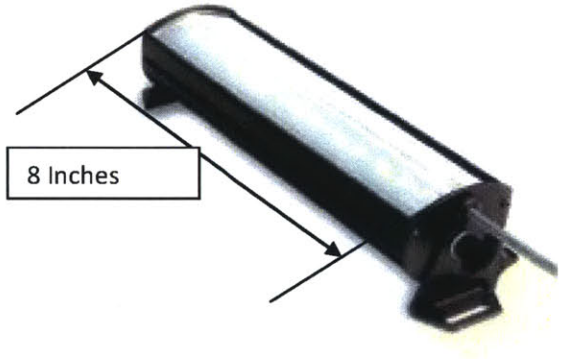

Figure 20: Figure showing LED illuminator used ("Metaphase ISO-8-IR-24")

4.4.3 Software

The image processing software is used to do image segmentation and identify the defects in the heat spreader material.

Key considerations for selecting the software

1. The software should be able to detect bright and dark spots in an image.
2. The software should be able to locate the object in an image.
3. The software should be able to detect different shapes in an image.

The software being used for this application is "VeriSens Application Suite v2.4.1" as it has tools to locate an object in an image, segment image on the basis of the characteristics of its pixels and compare features of one image with other. All these tools were useful in detecting defects (See chapter 5 for details). The tools of this software can be put into three categories based on their application, i.e. Part location, geometry identification and feature comparison, and each are listed in Table 4, 5 and 6 respectively.

Part Location features:

Table 4: Table describing part location tools in the software [14]

Feature	Description
Part location on contours	Part location on contours Determines the location and rotational position of a part based on its contours.
Part location on edges	Determines the location and rotational position of a part from a single edge or two edges at right angles to each other.
Part location on circles	Determines the location and rotational position of circular parts.
Part location on text lines	Determines the location and rotational position of text within a working area. The text may change during this task

Geometry Identification features:

Table 5: Table describing geometry identification tools in the software [14]

Feature	Description
Distance	Determines the distance between two edges
Circle	Determines location, roundness and diameter in comparison to reference circle
Angle	Determines the angles between two edges
Count edges	Determines the number of edges along a tracing ray
Point position	Determines the coordinates of one point

Feature comparison:

Table 6: Table describing feature comparison tools in the software [14]

Feature	Description
Count contour points	Determine the number of contour points within a working area
Contour comparison	Compares the contour of a taught in part with the contour of taught in part.
Brightness	Determines the average brightness in the working area
Contrast	Calculates the contrast in the working area
Area size	Determines the areas of bright or dark regions in the image. Determines the total area of the largest continuous area.
Count areas	Counts the continuous bright or dark regions visible in the image area.
Pattern comparison	Compares the working area with a taught-in pattern.

4.5 Experimental setup

The goal of the experiments is to be able to identify all the defects in the heat spreader material using the equipment described in the previous section. In order to achieve the desired goal, following parameters and their effects are to be investigated:

1. The position of heat spreader material with respect to the camera.
2. The position of lighting source with respect to the heat spreader material.
3. Camera exposure time while capturing an image.
4. Edge detection Sensitivity.

These parameters have a direct impact on the ability of the image processing software to detect a defect in an image. Thus, the experimental setup has to be designed to achieve the desired goal.

4.5.1 Camera Position

The position of the camera determines the area of the heat spreader material that can be captured in an image. The goal is to be able to capture the full area of the heat spreader material in an image. Keeping this in mind, the camera was fixed in a position so that the optical center of the front lens of the camera is parallel to the top surface of the heat spreader material and the distance (g) between the front lens and top surface of heat spreader material is greater than 450mm. The distance g is determined by using the basic lense equation 1 [22].

$$g = f' * \left(\frac{G}{B} + 1\right) \qquad \textit{Equation (1)}$$

1. Focal length of the lens used (f') = 8mm
2. Size of the camera sensor (B) = 4.8mm
3. Length of the heat spreader material (G) =265mm

Figure 21 is a visual interpretation of the parameters explained above.

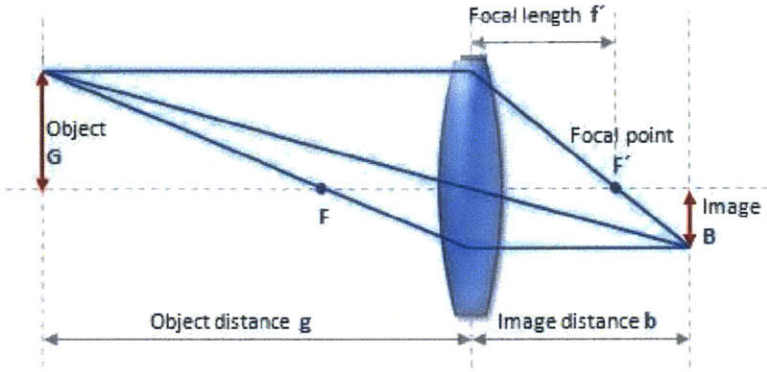

Figure 21: Figure showing optical path of a convex lens [22]

The Camera position is kept fixed at 530 mm in order to include the edges of the heat spreader material and also to accommodate for the size variation in the sheet (Figure 22). The camera position is fixed irrespective of the defect being analyzed.

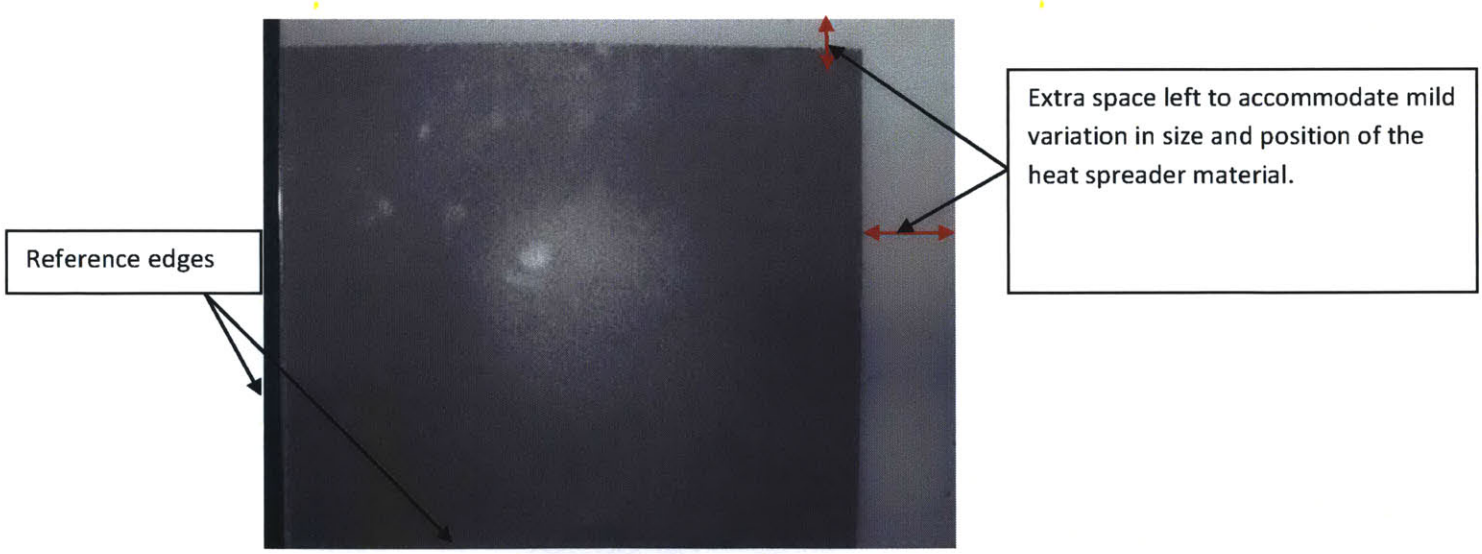

Figure 22: Figure showing image of heat spreader material captured by the camera.

4.5.2 Lighting Position

The position of the light directly impacts the quality of an image and also determines the detection ability of a particular defect. The position is determined in order to achieve maximum possible distinctness of a defect in an image.

Backlight: The heat spreader material is placed over the backlight leaving no distance between the backlight and material.

LED Illuminator: The position of the LED illuminator is varied according to the type of defect for which the material is being analyzed. (See chapter 5 for details)

The camera used detects both infrared and visible light. In order to avoid any hindrance from the visible light from the environment, all the experiments were done in a dark room environment.

4.5.3 Camera exposure time

Camera exposure time determines the amount of time for which the camera sensor is exposed to light before capturing an image [25]. It has an impact on the quality of an image and distinctness of the different features of an image. It is measured in microseconds. The higher the exposure time, the more is the loss in important details of the image. The loss in details is caused by the large amount of light entering the camera sensor and it appears as bright spots in an image [25]. The goal while taking an image is to keep exposure time at a minimum required level to capture all the relevant features in an image. If the exposure time is very low, some features of the actual objects become invisible due to lack of the amount of light reaching the camera sensor. The camera exposure time is varied according to the defect being analyzed in order to achieve maximum possible distinctness in the visibility of the defect in an image.

4.5.4 Edge detection sensitivity

The edge detection feature determines the contours in an image, i.e. points where there is a significant change in intensity as compared to its immediate surroundings. It is measured in percentage (varies from 5 % to 100%). The higher the edge detection sensitivity, the less is the possibility of noise in an image. (See Figure 23)

Noise in an image refers to those pixels in an image which have intensity difference from its immediate surroundings less than the maximum possible value and are detected as contours.

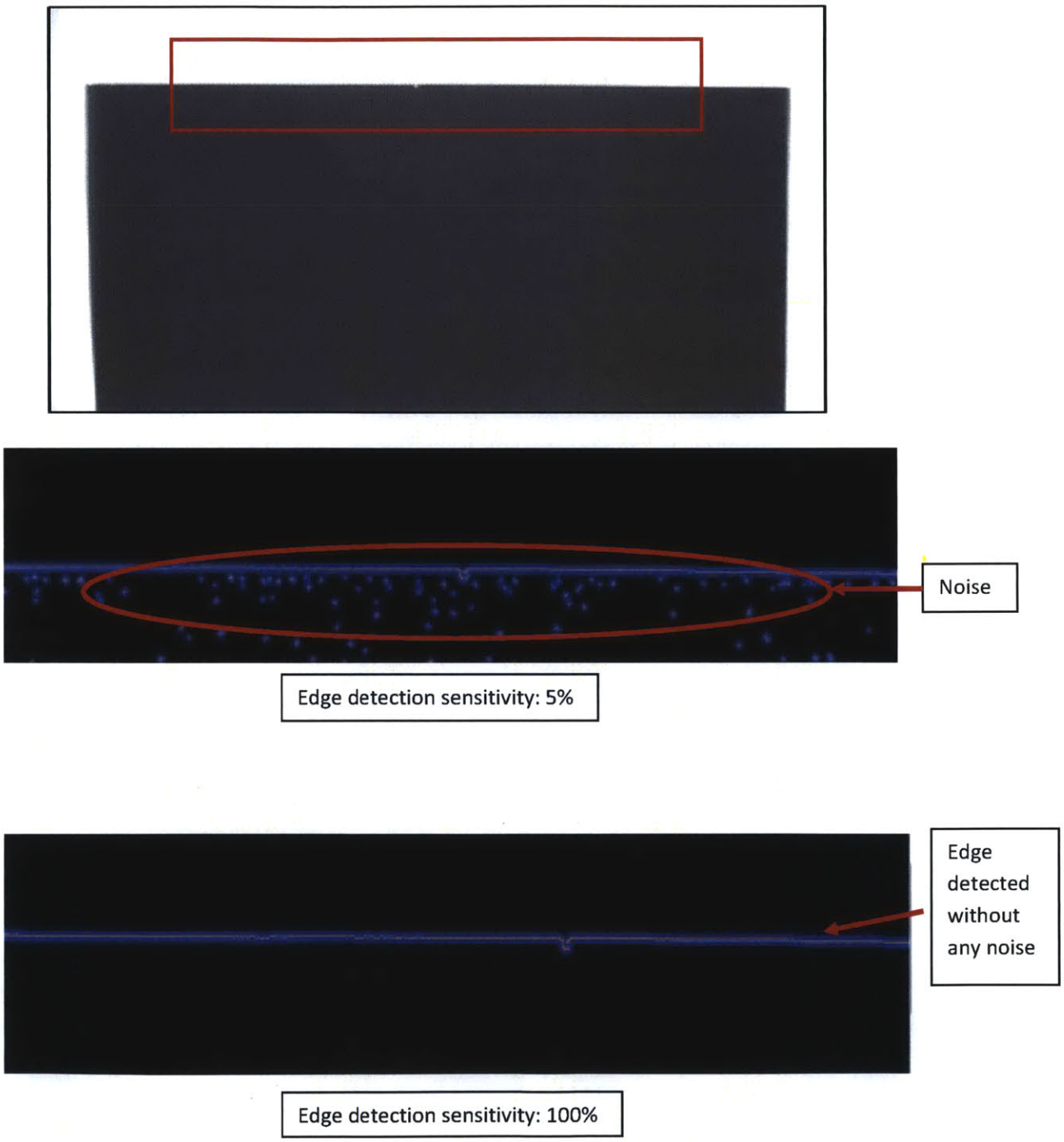

Figure 23: Figure showing noise level in an image at different sensitivity level

Chapter 5. Design of Experimental Setup

5.1 Overview

This chapter explains the approach taken to determine the best light, camera and software parameters to conduct the experiments for detecting a particular defect.

5.2 Design of Experimental setup

Since different parameters are relevant to different defects, the different experiment designs are explained according to the defect.

5.2.1 Chromic Aberration

Principle of the experiment

The surface texture of the area having chromic aberration is different from the rest of the sheet, i.e. the surface of the sheets having chromic aberration shows more characteristics of carbonized sheets because sheets having chromic aberration are not fully converted to graphitized sheets. As it can be observed in Figure 24, the carbonized sheets are shinier than graphitized sheets i.e. it is dominated by specular reflection whereas the property of the graphitized sheets is more dominated by diffused reflection.

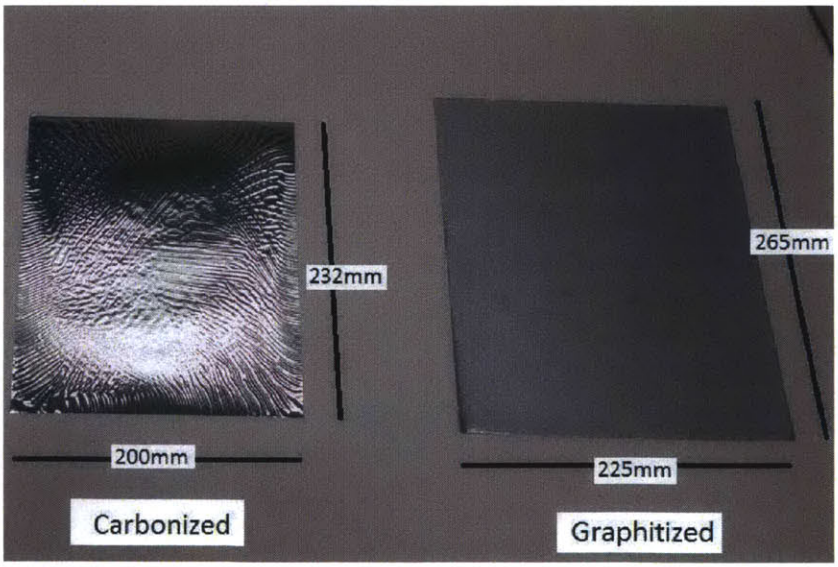

Figure 24: Figure showing carbonized sheet and graphitized sheets. It can be observed that carbonized sheets diffuses less light.

The above mentioned characteristic of chromic aberration was useful in detecting the defect. When pictures of the two different sheets were taken, the images of sheets having chromic aberration appeared to be more shiny when compared to the images of normal sheets which can be observed in figure 25. The number of bright points in an image can be counted using a software tool, so ideally sheets having chromic aberration should show a higher number of contour points (bright spots in a sheet) as compared to the normal sheets.

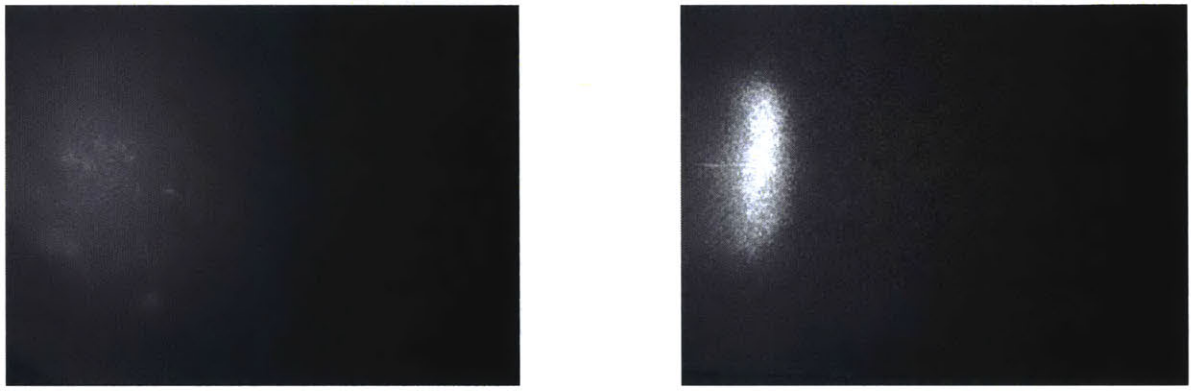

Figure 25: Left image is of the sheet without chromic aberration and right image is of the sheet having chromic aberration (Surface of sheet without chromic aberration absorbs more light when compared to surface of sheet with chromic aberration).

Parameters of Experiment

Lighting position: The backlight was not significant in the determination of this defect so it was not used. The LED illuminator was positioned parallel to the surface of the heat spreader material with distance (D) of 440 mm between the plane containing the light source (Plane A) and plane containing heat spreader (Plane B) (See Figure 26).

The distance (d) between plane perpendiculars to Plane B and containing the edge of the sheet nearest to the light source (Plane C) and the plane parallel to plane C and containing the center of the LED illuminator (Plane D) was set at 100mm.

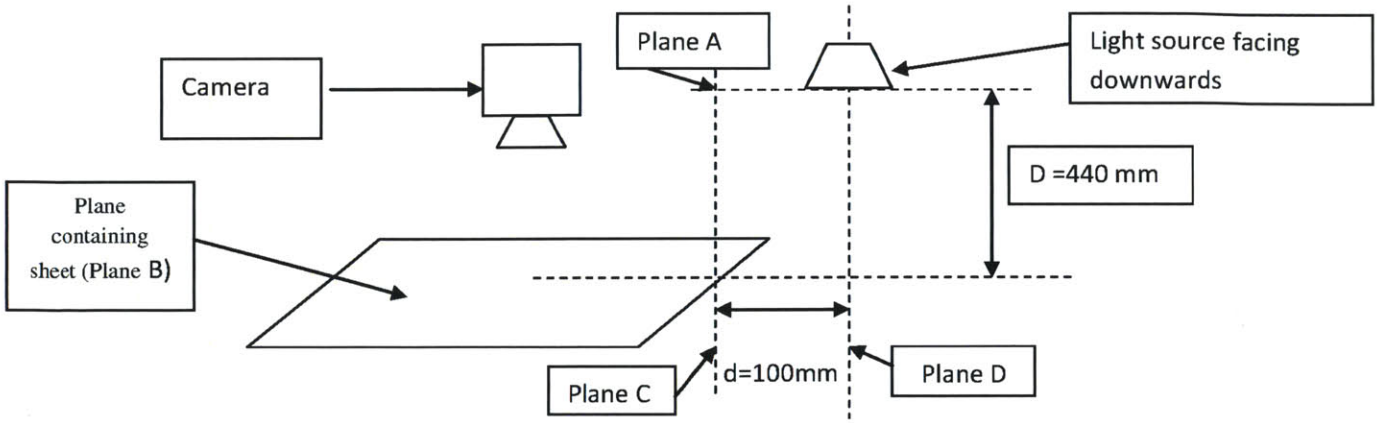

Figure 26: Figure showing Experimental setup for testing chromic aberration

Distance (d) is maintained greater than 0 because the heat spreader material has reflective properties, so distance d is varied until the image of the light itself is not visible on the surface of heat spreader material. The image of the light on the heat spreader material would create noise in the image (that part would appear to shine thus hiding features of the sheet, see figure 27).

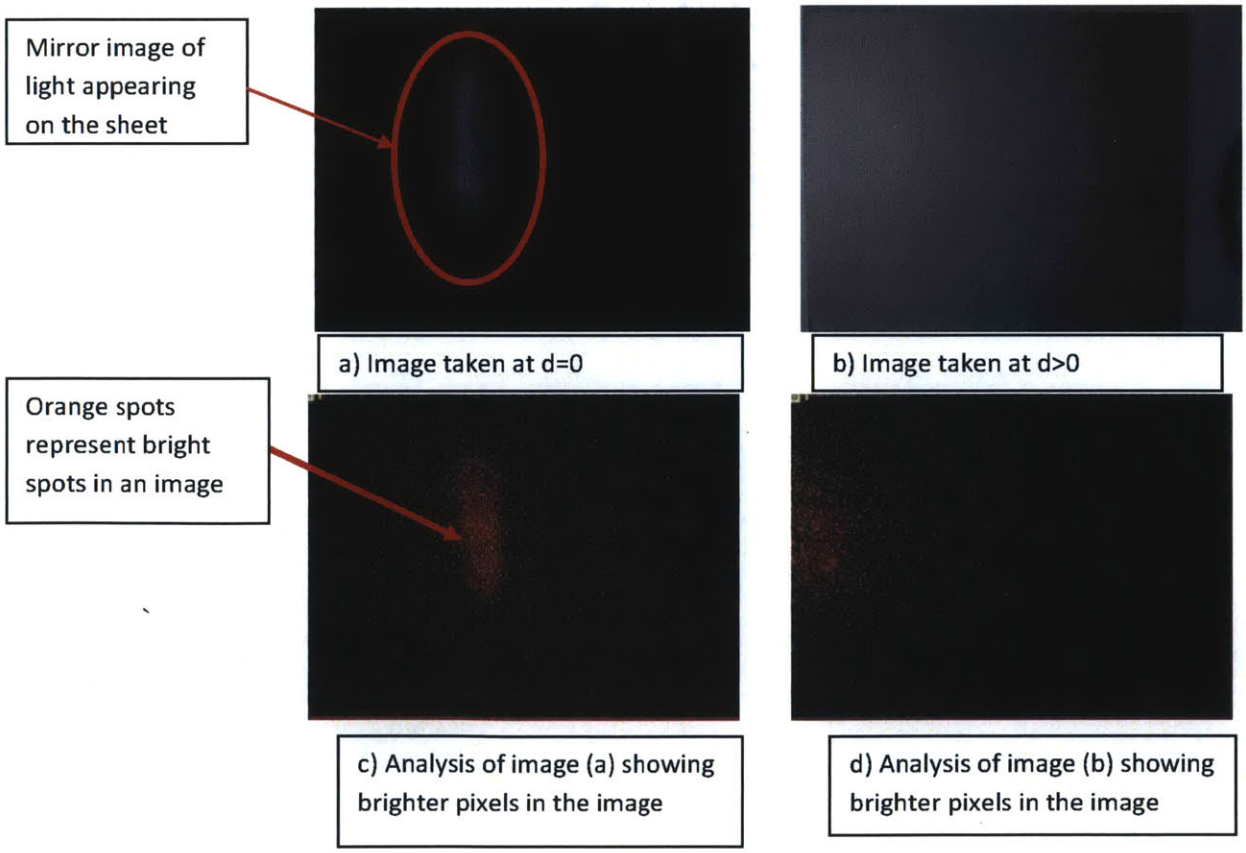

Figure 27: Figure showing effect of lighting position with respect to heat spreader material on the image processing.

Exposure time: The exposure time has to be maintained at a level that ensures capturing of features required to detect chromic aberration (refer section 4.5.3). So experiments were done with sheet having chromic aberration concentrated in a small area in the center of the sheet (Figure 28).

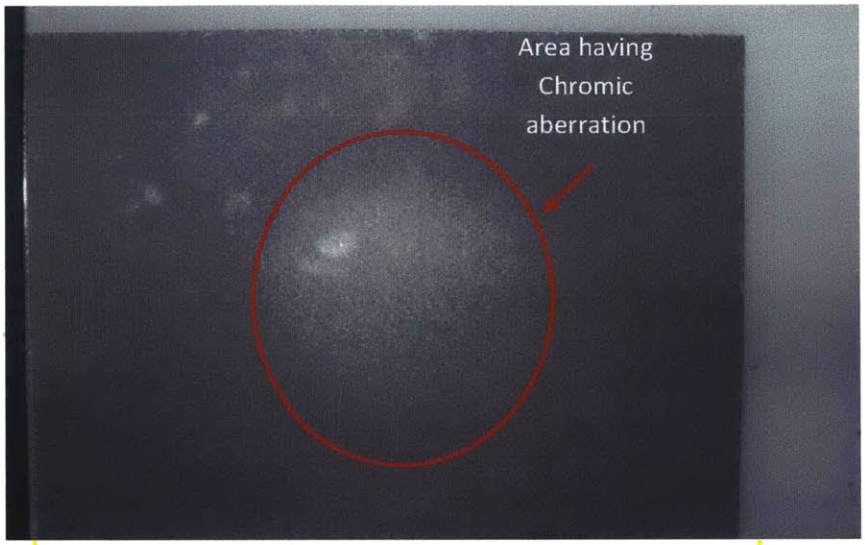

Figure 28: Image of sheet used to determine exposure time

Since chromic aberration is always present at the center of the sheet, it was a prime requirement that the features of the center of the sheet are visible in an image.

As it can be observed in figure 29, at a higher exposure time the center part of the sheet having chromic aberration is visible, but is not at all visible at a lower exposure time.

Based on these tests the exposure time was determined to be 500 µs.

Note: Higher or lower exposure time than 500 µs can also be chosen if the required features are visible in an image. For the simplification of the experiment, exposure time was fixed at 500 µs as it was fulfilling the minimum requirement needed for this experiment.

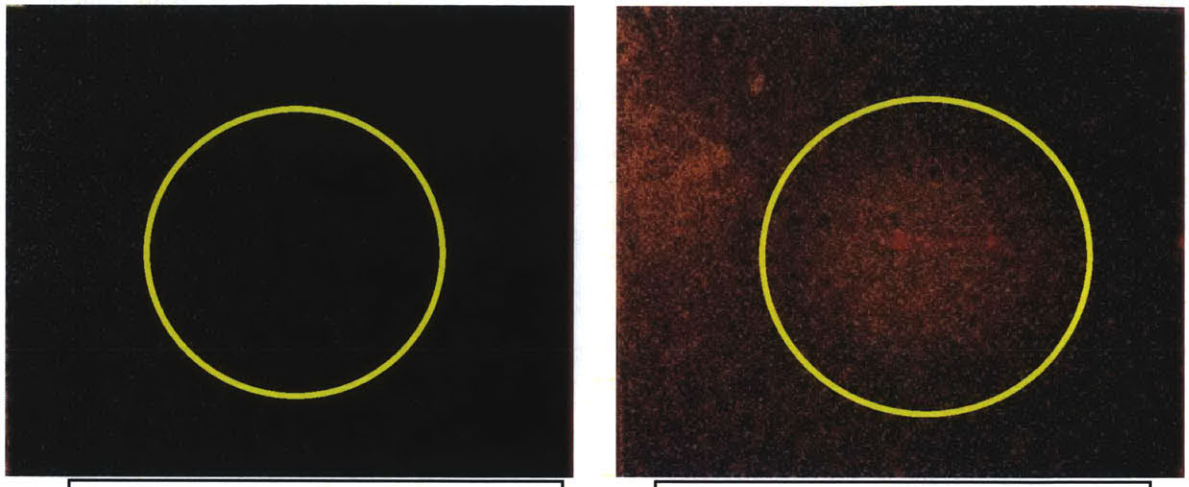

Figure 29: Figure showing analysis of image of a same sheet taken at different exposure time

Edge detection sensitivity: As explained in section 4.5.4. At lower edge detection sensitivity image will show a higher number of contour points, which is a favorable condition for detecting chromic aberration. Thus, the edge detection sensitivity is set at the lowest possible value, i.e. 5%.

Software Tool: The tool used to determine and quantify chromic aberration is called " Count contour points" (See table 6). This tool counts the number of points that higher intensity as compared to the rest of the image. Since the sheets having chromic aberration reflect more light as compared to normal sheets, the number of bright points in its image is more than that in an image of a normal sheet.

5.2.2 Distorted edges

Principle of the experiment

Sheets having distorted or broken edges, when placed in front of a light source will block the light except for the areas that are broken. This property can be used to detect the shape of the edge of the sheet and then can be compared to the edges of the good sheets.

Experimental Setup

Lighting position: The heat spreader material is placed on the surface of the backlight.

Exposure Time: The exposure time was decided on the basis of sharpness of the image. The goal is to get the maximum possible contrast between the object and its background so that edges of object are clearly visible in an image. Experiments were conducted to measure the contrast at various levels of exposure time. The relationship between exposure time and contrast value of the image is shown in Figure 30.

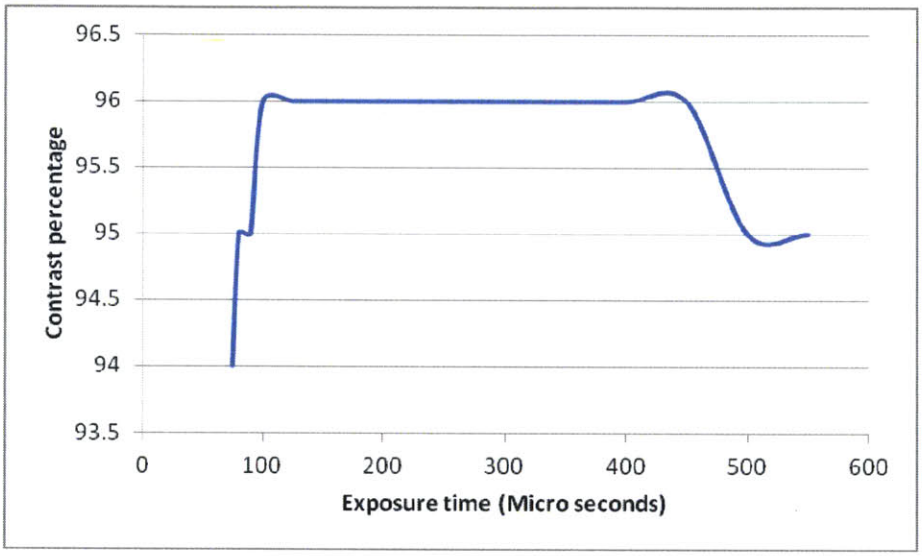

Figure 30: Figure showing relationship between contrast percentage and exposure time.

As it can be observed in figure 30, the maximum contrast percentage that can be achieved is 96%. Based on this result and on the quality of image achieved, exposure time was set at 300μs.

Edge detection sensitivity: For the application of detecting an edge, noise from within the sheet is not acceptable, so edge detection sensitivity was fixed at 100% so that no noise is there in the sheet.

Software tool: Two software tools are used to detect the distorted edges. One is "part location on edges"(see table 4) to determine the location of the edge of the sheet in an image, and another is "contour comparison" (See table 6) to compare the contour pattern of the normal sheet with that of the defective sheet.

5.2.3 Holes

Principle of the experiment

The heat spreader material is opaque; hence when placed in front of a light source, any holes or missing areas will show up as white spots on the dark sheet (See Figure 31). Such bright spots in an image can be identified by the software as the contrast between these spots and rest of the image is very high.

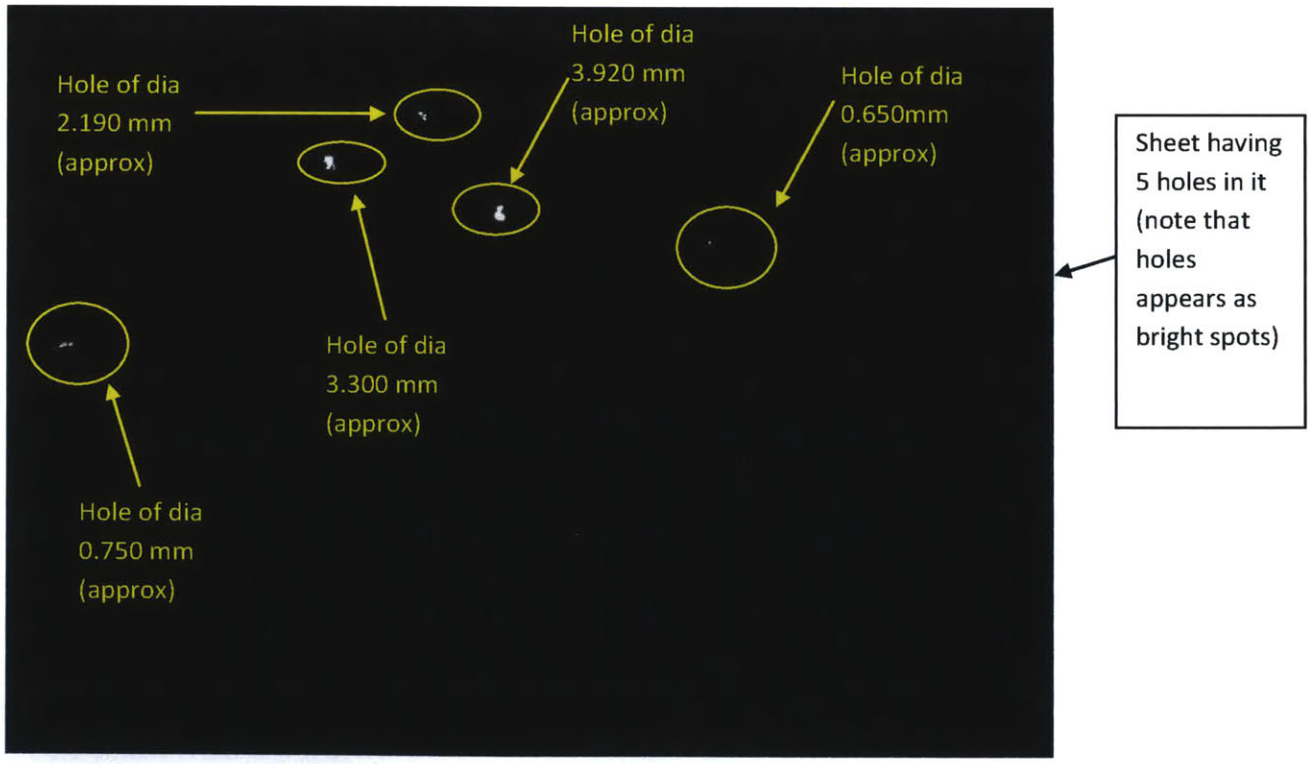

Figure 31: Figure showing holes as captured in an image. The encircled areas represent holes in a sheet.

Experimental Setup

The lighting, exposure time and edge detection sensitivity were kept the same as for the distorted edges since the same principle applies to detection of holes. (See section 5.2.2)

Software Tool: The software tool used for detecting holes is "count areas."(see table 6). This tool counts the number of dark areas on bright object or bright areas on the dark object. In our case, we will use it for counting bright areas on the dark object (See figure 31).

Other components of this tool:

1. Binary threshold: It sets the threshold value of pixel intensity level. For example, if the binary threshold value is set at 200, then pixel having an intensity level more than 200 would be classified as bright areas and the pixels having an intensity level lower than 200 would be classified as dark areas. It varies from 0 to 255. In our case, it is set at the maximum possible value value (255) because the contrast between holes and sheet is at the maximum level.
2. Area Filter: It adjusts the number of pixels, to be considered as a single area (it varies from 0 to 1000). In our case, the minimum value is set at 0 in order to be able to detect the smallest possible hole and maximum is set at 1000 in order to be able to detect the largest possible hole in dia.

5.2.4 Spots

Principle of the experiment

The spots in the sheets are shinier than the rest of the surface because of the area of spot is the area which is not fully converted to the graphitized sheet. They appear distinctly in the image as there is sufficient contrast between spots and the rest of the image. The reason for the distinctness of spots is same as chromic aberration with only difference is that the spots are limited to small areas of the sheet. It is this property that can be used to detect the spots (See Figure 12 in section 3.2.4).

Experimental Setup

Lighting position: The lighting setup used to detect spots is same as the one used for chromic aberration except for one change, i.e. distance (d) is set at 33 mm. Refer Figure 26 for the setup. This setup is used because in order to detect spots, light should be directly incident on the surface of the sheet exposed to the camera which is the same case with chromic aberration.

The distance d is maintained to ensure the light falls directly on the sheet as spots get detected when light directly falls on them. To identify the area where light would be incident directly on the sheet, a glass plane was used to capture the image of the light and define the area where light would fall directly on the sheet (See Figure 32). Later it was ensured that the spots to be checked lie in the defined area.

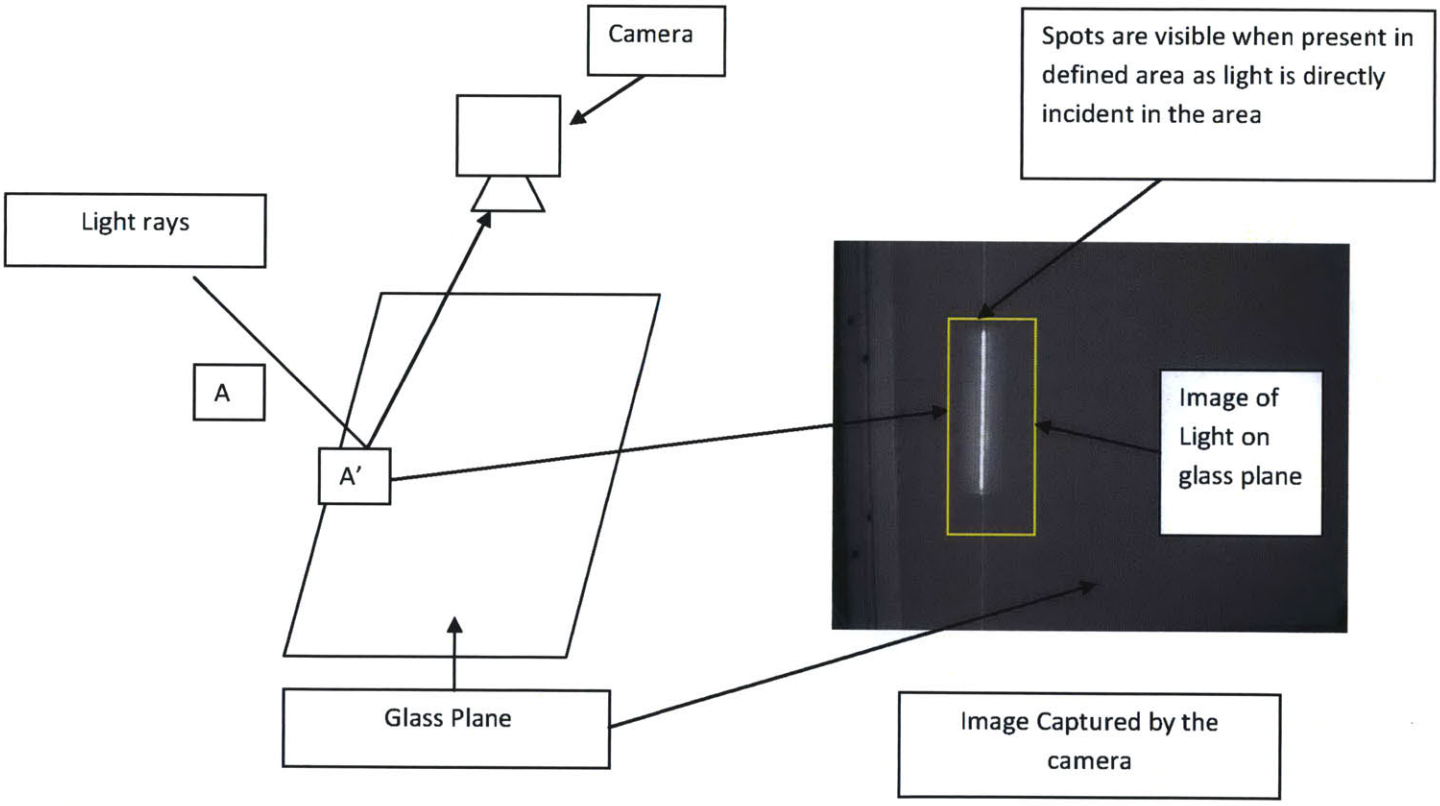

Figure 32: Figure showing area where spots can be detected

Exposure Time: The exposure time was set at 760 µs as at this exposure time, spots were visible without the noise from the surrounding area.

Edge detection sensitivity: In order to keep image noise at optimum level, edge detection sensitivity was set at 35%. This value was selected by observing sheets at different edge detection sensitivity values and identifying a value where software could identify spots.

Gamma correction: The gamma correction feature balances the brightness in the image, i.e. it reduces the brightness concentrated in the small area of the image and spreads it to darker areas. The gamma correction feature was enabled for this application (See Figure 33).

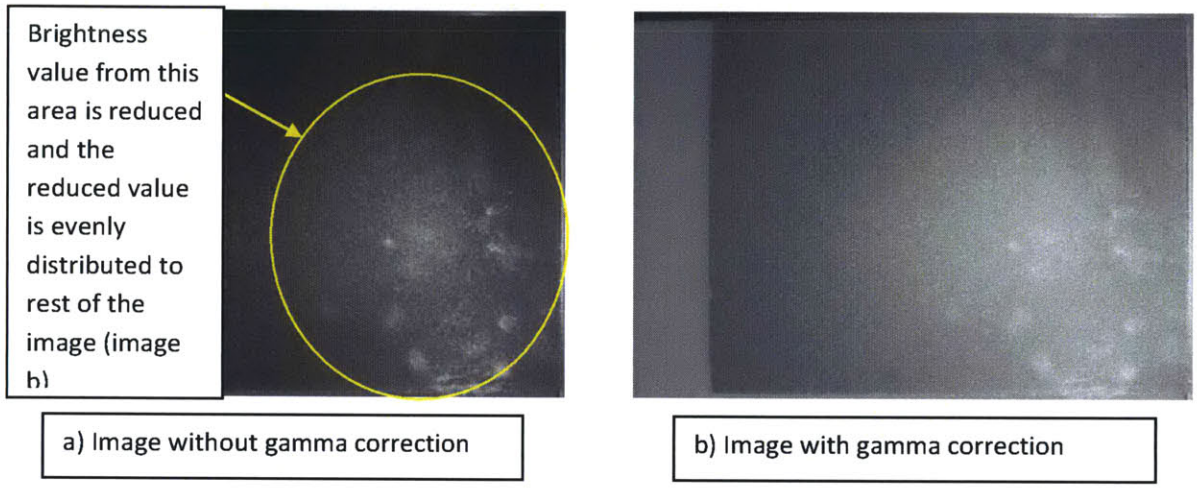

Figure 33: Figure showing comparison of image with gamma correction to image without gamma correction when all the other parameters were kept same

Software Tool: The software tool used for detecting spots is "count areas." (See table 6) This tool counts the number of dark areas on bright object or bright areas on the dark object. In our case, we will use it for counting bright areas on dark object.

Other components of this tool:

In order to select a binary threshold and area filter value, the following approach was taken:

Since in the case of spots, the contrast is not very high, so the sheets were visually inspected and four sheets were shortlisted in which the spots were not too shiny, i.e. hard to find as compared to the entire population and were tested for different combinations of area filter and binary threshold values.

The target of this test was to find out a combination of values of binary threshold and area filter at which all the spots present in the defined area are detected, and no noise is detected.

In general, by increasing the area filter and binary threshold, the error decreases in value, but increasing both the values too much might lead to negative error.

The error is defined by equation 2

$$Error = \frac{Spots\ detected - actual\ spots}{Actual\ Spots} * 100\% \qquad \text{Equation (2)}$$

A negative error means that less number of spots are detected than actual and a positive error means that a higher number of spots than actual are detected.

Based on the analysis of these four sheets, the binary threshold value was set at 120 and area filter value was set at 8. At these values, there was noise in one sheet. At values lower than 120 and 8, a higher positive error was observed in other sheets and at values higher than this, a negative error was observed. Since the negative error is absolutely unacceptable, the binary threshold value and area filter value was set at 120 and 8 respectively.

5.2.5 Angled Edges

Principle of the experiment

The image captured by the camera is divided into pixels. The position of any point in a two dimensional image can be located by the pixels in the x coordinates and y coordinates. This image coordinate system can be converted into user defined coordinate system and the position of two corners of a well defined edge can be located.

An image of graph paper is used as reference to convert the image coordinate system into a user defined coordinate system (See Figure 34).

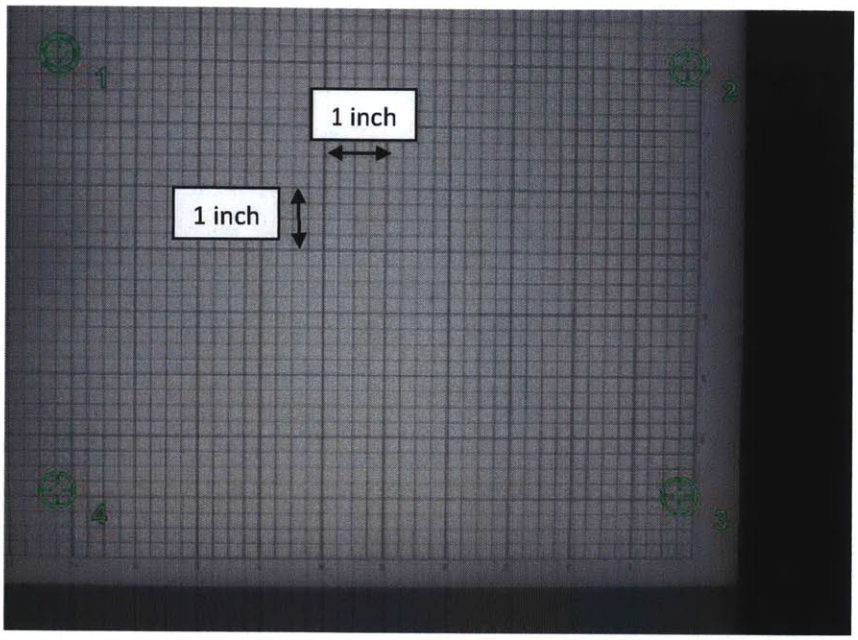

Figure 34: Figure showing image of the graph paper used as reference to define coordinate system

The default coordinates of the image (Figure 34) are converted as shown in table 7:

Table 7: Table showing coordinates conversion from pixels to inches

Point Number	Original coordinate		Converted coordinate	
	X value (pixels)	Y Value (pixels)	X value (inches)	Y value (inches)
Point 1	81	79	0	0
Point 2	1028	79	10	0
Point 3	1028	742	10	-8
Point 4	0	742	0	-8

Experimental Setup

The lighting, exposure time and edge detection sensitivity were kept the same as for checking distorted edges since the same principle applies to detection of angled edges. (See section 5.2.2)

Software Tool: The software tool used for detecting this defect is called "point position" (See table 5). This software tool can be used to locate the position of two points through which distance between them is calculated.

Chapter 6. Results and Conclusions

6.1 Overview

This chapter explains the methodology followed for each experiment, the results and what can be concluded from the results.

The experiments were different for different types of defects and are explained according to the defect.

6.2 Chromic Aberration

6.2.1 Experiment methodology

The sheets having chromic aberration were categorized into four levels. The difficulty in detecting chromic aberration decreases with an increase in level. Level 1 sheets are considered to be non defective, level 2 are borderline cases (can be easily missed by an inexperienced worker). Sheets above level 2 are considered defective. The sheets were categorized based on the judgment of the worker who inspects the material.

Since chromic aberration was always present at the center, only the contour points in a small area in the center of the sheets are counted. The Center of the sheet can be found out by locating coordinates of the four corners of a sheet in the image.

In order to decide on the area, a sheet having chromic aberration spread over the smallest area of the surface was captured in an image. (See figure 35). Then the diameter (d_1) of the spread of chromic aberration was measured in the image and a circular area having a diameter (d_2) less than d_1 was selected to count the number of contour points.

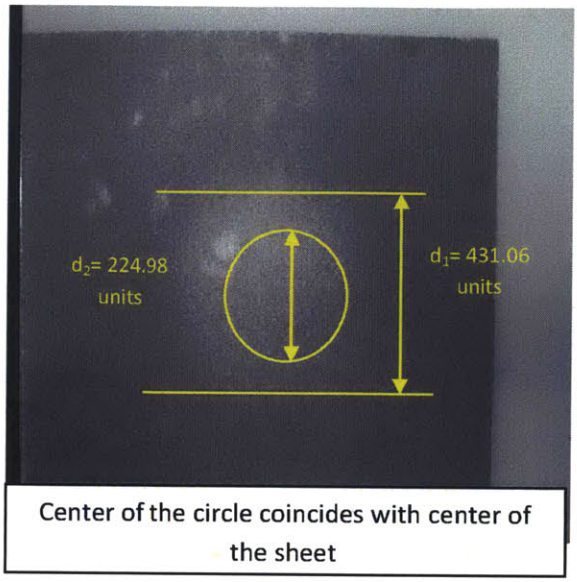

Figure 35: Figure showing area selected to count number of contour points.

The position and the area in an image where the contour points were counted was kept same throughout the experiment.

6.2.2 Results

Five samples of the sheets within each level were taken, and the results are shown in table 8. The level of sheets was determined by experienced operators inspecting the sheets. A total of 20 sheets were measured.

Table 8: Table showing number of contour points observed for different levels of Chromic aberration

Sample number	Number of Contour points			
	Level 1	Level 2	Level 3	Level 4
Sample 1	5485	8357	6325	7657
Sample 2	5591	7784	6571	7917
Sample 3	5676	7447	7441	8608
Sample 4	6033	7661	7961	9341
Sample 5	5796	7932	8108	9081

AVERAGE	5716.2	7836.2	7281.2	8520.8
STANDARD DEVIATION	210.64	341.06	804.67	725.42
COEFFICIENT OF VARIATION	0.037	0.04	0.11	0.08

The results are shown graphically in Figure 36.

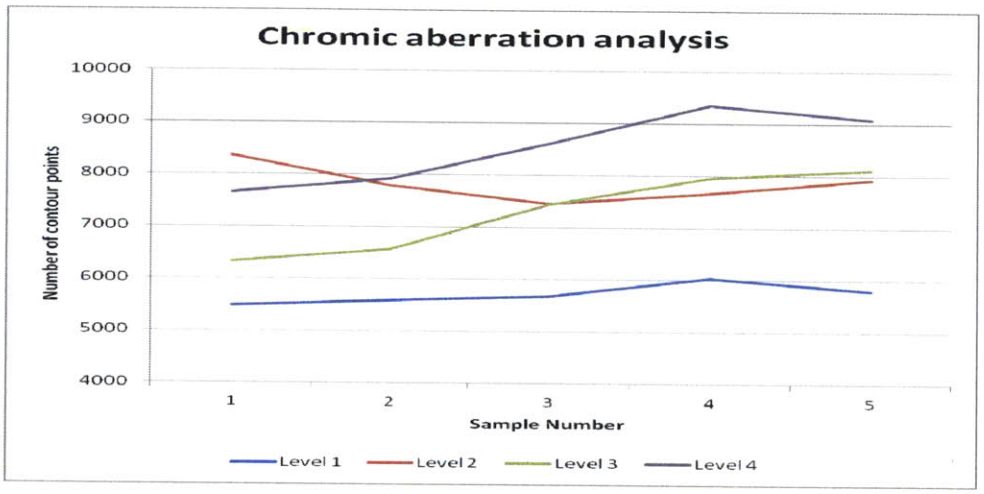

Figure 36: Figure showing analysis of sheets having different levels of chromic aberration.

6.2.3 Conclusions: Chromic aberration

We can conclude from the results that good sheets can be separated from defective sheets with very high precision as standard deviation is very low. (See table 8). The high coefficient of variation in the defective sheets can be attributed to human factors, as it was observed that inexperienced workers can easily mix sheets with the chromic aberration of level 2 and level 3 (see figure 34), as level 2 sheets are borderline cases and also sometimes level 2 sheets can be mistaken with good sheets. By installing the automatic vision system, this error can be removed.

It was also observed that one set of samples which was classified as level 2 chromic aberrations had a number of contour points of the order of level 4 sheets. (See Table 9)

Table 9: Table showing number of contour points observed in samples that were wrongly classified

Sample number	Number of Contour points
Sample 1	8332
Sample 2	8387
Sample 3	8583
Sample 4	8400
Sample 5	8373
AVERAGE	8415
STANDARD DEVIATION	97.32163
COEFFICIENT OF VARIATION	0.011565

This human error can be attributed to the fact that the chromic aberration in this sample set was uniformly distributed over the whole area so it was difficult to detect.

The number of contour points in a sheet is also dependent on the input material used to produce heat spreader material and other input parameters of the manufacturing process, but within a particular batch, the sheets having chromic aberration will always show a higher number of contour points than the normal sheets. For example Sheets having different levels of chromic aberration were chosen from two different batches, one manufactured in the year 2013 and another in the year 2014 to observe the number of contour points in them. These sheets had different characteristics as for their processing a different input material was used in both the case. The results obtained from the observation of contour points are shown in Figure 37.

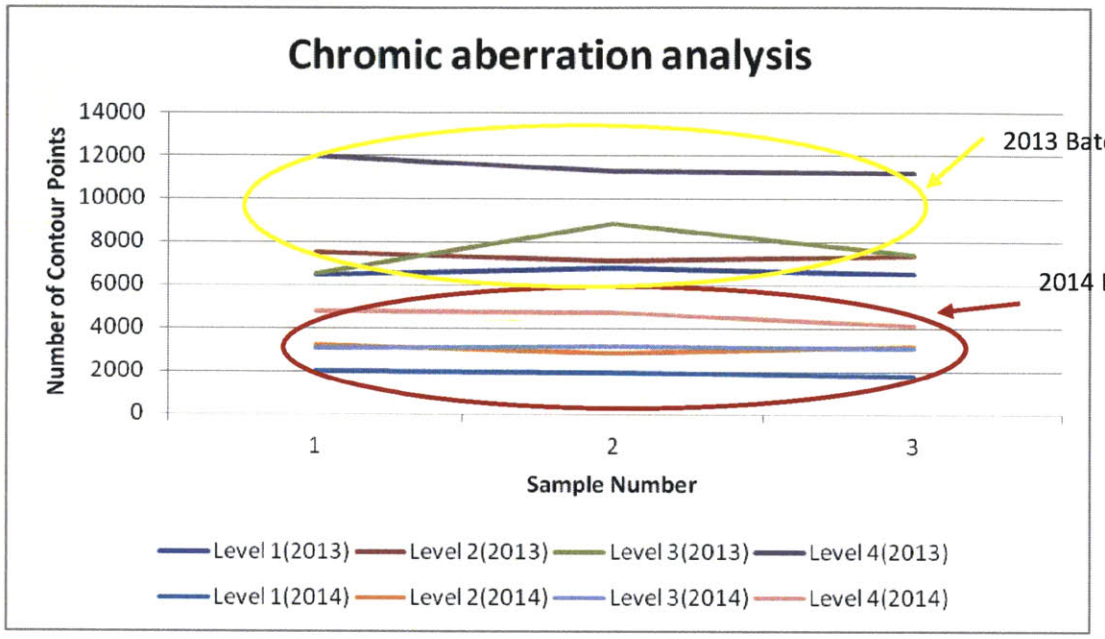

Figure 37: Figure showing chromic aberration analysis of two different batches of sheets.

6.3 Distorted Edges

6.3.1 Experiment methodology

First, a sheet without any edge distortion is selected and the image of this sheet is taken. Using the edge detection tool, its edge is located and the contour pattern of its edge is recorded (See Figure 38). Then samples of both good and defective sheets were taken, and their edges were compared with the contour pattern recorded in the software. The similarity in patterns is measured in terms of percentage of pixels in the observed area of the image that is similar to the pixels in recorded pattern. Ideally, the sheets with distorted edges should not match with the recorded contour pattern, i.e. the percentage of similarity should be very less when compared with the results of good sheets.

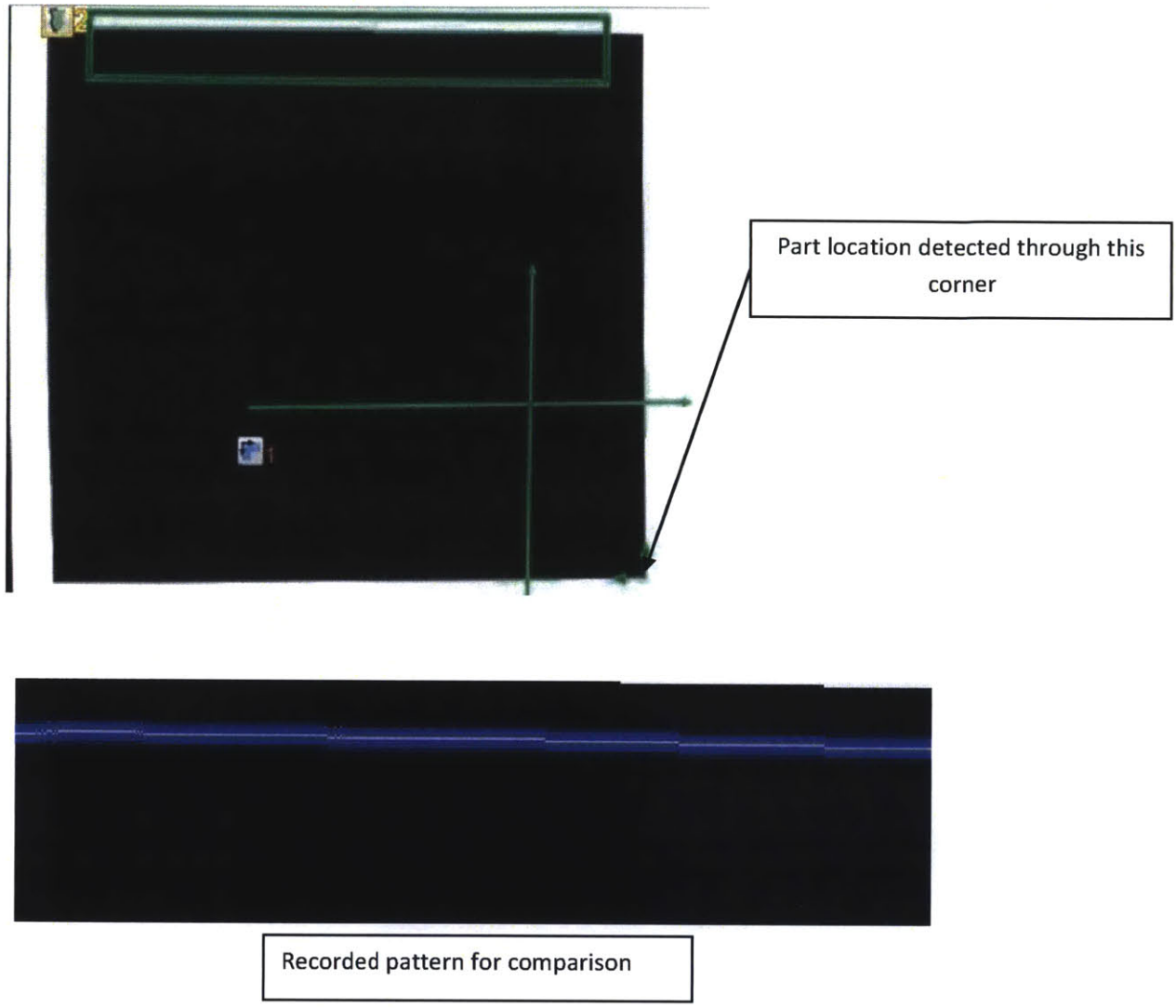

Figure 38: Figure showing setup for detecting distorted edges

6.3.2 Results

Good Sheets

The edge pattern of sheets having edges without any distortion were compared to the recorded pattern. The results obtained from this comparison are listed in Table 10.

Table 10: Table showing correlation between good edges and recorded edge pattern

Sample Number	Correlation percentage
Sample 1	99%
Sample 2	100%
Sample 3	100%
Sample 4	100%
Sample 5	100%

Defective sheets

The edge pattern of sheets having distorted edges was compared to the recorded pattern. The results obtained are listed in Table 11.

Table 11: Table showing correlation between bad edges and recorded edge pattern

Sample Number	Correlation Percentage
Sample 1	94%
Sample 2	0%
Sample 3	96%
Sample 4	12%
Sample 5	97%

The variation in correlation percentage can be related to the amount of distortions at the edge (See Figure 38). As it can be observed in the figure 39, Sample 1, 3 and 5 have straight edges, but a minor break is at the edges where as edges in sample 2 and 4 are not even straight.

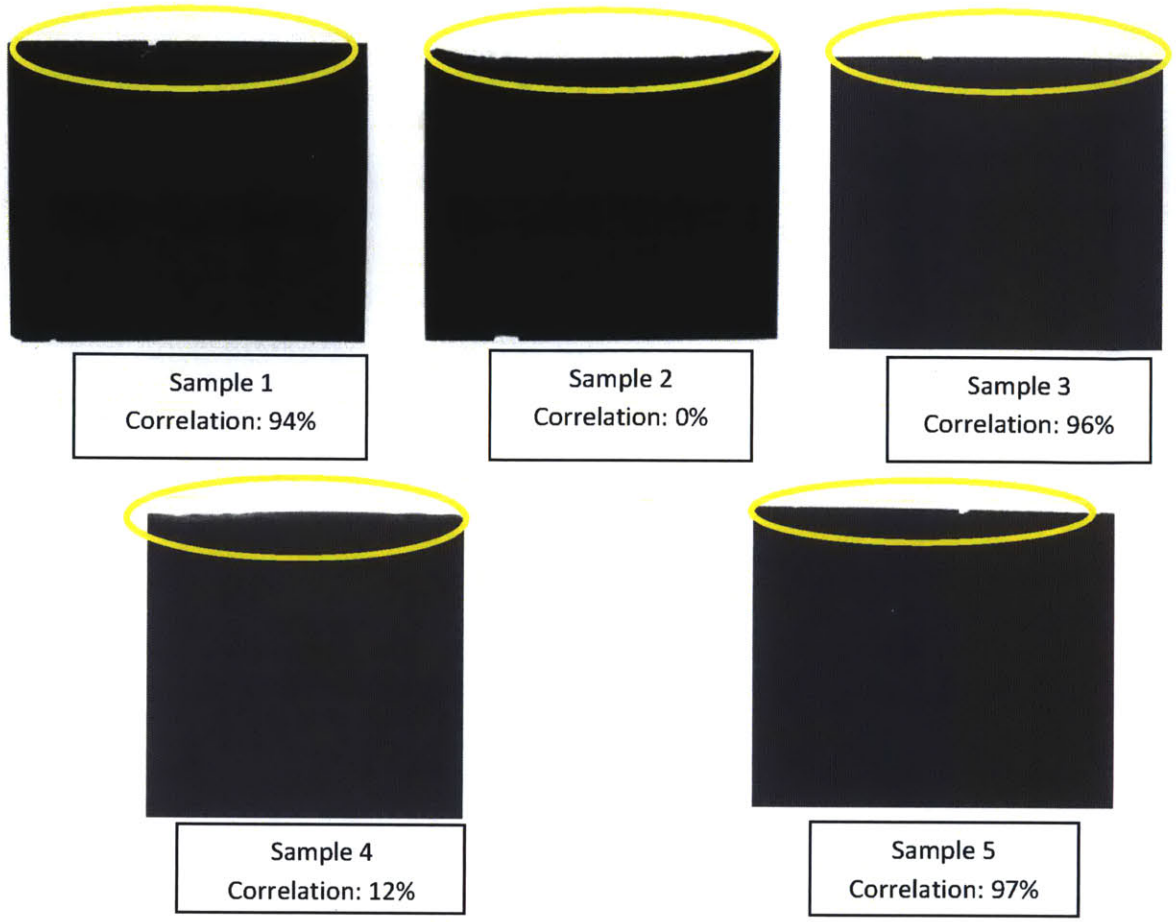

Figure 39: Figure showing edges of defective samples that were tested

6.3.3 Conclusions: Distorted Edges

The experiment proves that contour comparison tool can be used for comparing edges of the sheet and the amount of distortions is reflected in correlation percentage, so tolerance can be set according to the requirement. It can be deduced from the results of this experiment that sheets having distorted edges have correlation percentage less than 99%.

6.4 Holes

6.4.1 Experiment methodology

A sheet with five holes of different diameters was tested under the recommended setting to see if the software tool could detect all the holes (See figure 40). One normal sheet was also tested under the same settings to confirm that the software does not show any error in judgment.

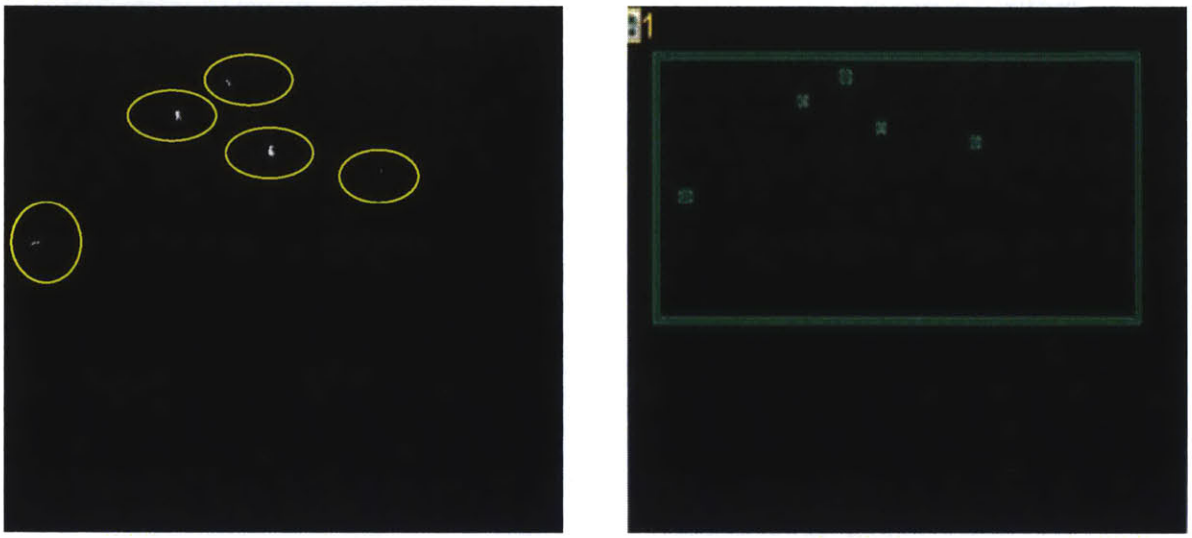

Figure 40: Image on left is of the sheet which was tested and image on right shows the marks where software detected a hole

6.4.2 Results

The results obtained from the experiment done to detect holes are listed in table 12

Defective sheets:

Table 12: Table showing results of experiment done to detect holes

Diameter of hole	Detected by software
0.650mm	Yes
0.750mm	Yes
2.190mm	Yes

3.300mm	Yes
3.920mm	Yes

Good sheets: No hole or noise was detected.

6.4.3 Conclusions: Holes

The sheets having holes can be detected by the software with very high accuracy. The smallest hole detected by the software was having a diameter of 650 microns.

6.5 Spots

6.5.1 Experiment methodology

The area where the image of light was captured was marked and twenty sheets having spots were studied under the camera. The different spots in a sheet were tested under the marked area by changing the position of the sheets to see if spots can be detected or not.

6.5.2 Results

The results obtained from the experiments done to detect spots are listed in table 13.

Table 13: Table showing number of spots detected vs number of actual spots in a sheet

Sample Number	Number of actual spots	Number of spots detected	Error % $\left\lvert\frac{Spots\ detected - actual\ spots}{Number\ of\ actual\ spots}\right\rvert * 100\%$
Sample 1	1	1	0
Sample 2	4	8	100
Sample 3	4	4	0
Sample 4	1	1	0
Sample 5	1	1	0
Sample 6	1	1	0
Sample 7	1	1	0

Sample 8	1	1	0
Sample 9	1	1	0
Sample 10	1	1	0
Sample 11	1	0	100
Sample 12	1	3	200
Sample 13	1	0	100
Sample 14	1	1	0
Sample 15	1	1	0
Sample 16	2	2	0
Sample 17	1	1	0
Sample 18	1	1	0
Sample 19	1	1	0
Sample 20	1	1	0
Sample 21	2	2	0
Sample 22	1	1	0
Sample 23	2	2	0
Sample 24	2	2	0
Sample 25	1	1	0
Sample 26	2	2	0
Sample 27	2	2	0
		Average error	18.52%

6.5.3 Conclusions: Spots

Noise was detected in sample 2 and sample 12, which can be removed by adjusting the binary threshold and area filter levels, but this will also have an effect on other sheets and at other values, the software will not detect some spots in other sheets.

Sample 11 and sample 13 had wrinkles around the spot, so the spot was not visible in the image which means that the above methodology can fail to detect a spot if the contrast level

difference between spot and the rest of the sheet is very low and if the spot is not visible in the image due to any other distortion in the image.

This analysis can be more precise as more and more data are available as with more data, we can get more failure modes and can adjust the parameters accordingly.

This analysis is not useful to define the area of a spot as different spots have different contrast level and there is a slight shade difference within one spot, which hinders in defining the area of the spot.

6.6 Angled Edges

6.6.1 Experiment methodology

One edge of a sheet was used to observe the offset in the Y direction of the corners. One corner of the edge was kept at a fixed point and other corner was varied by tilting the sheets at different angles to take readings at different offset values. The offset was measured physically using a ruler of least count 1 mm and was compared with the offset calculated by the software (least count of 0.254mm). (See Figure 41)

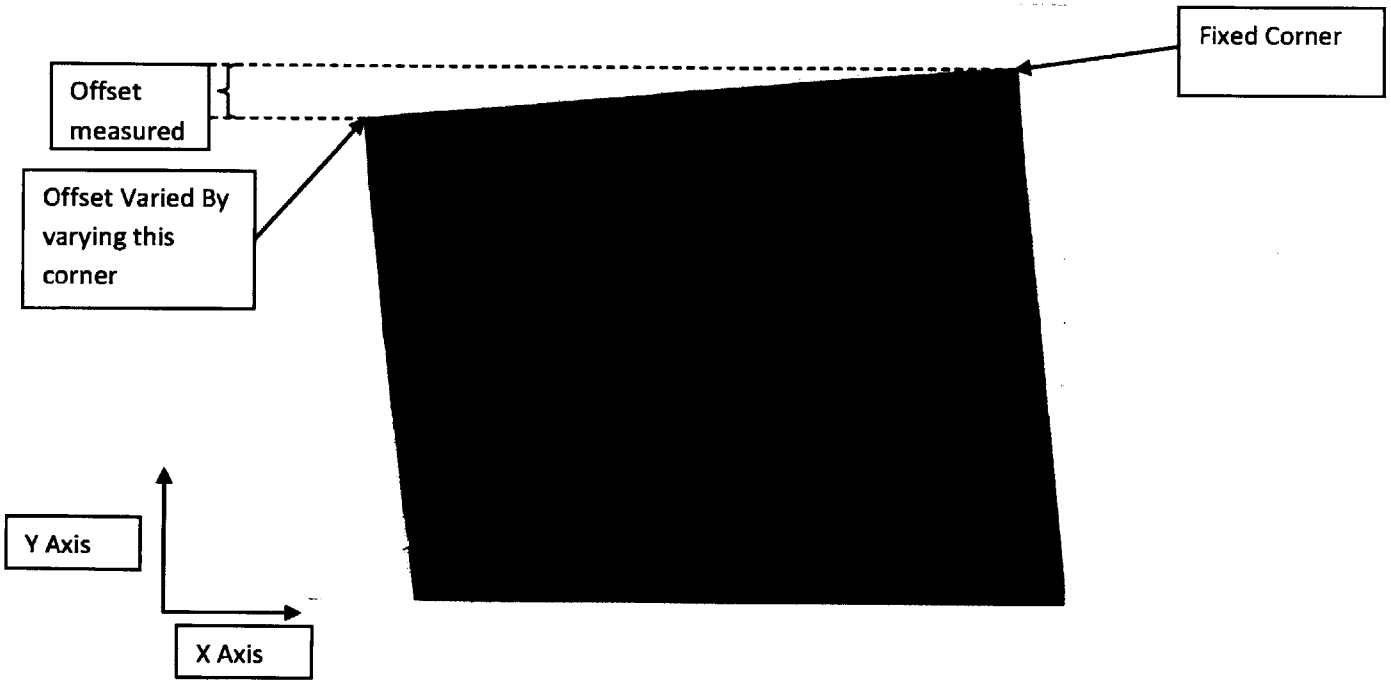

Figure 41: Figure showing experiment methodology used to detect angled edges

6.6.2 Results

The comparison of offset values measured by software to the values measured by ruler at five different angles of the sheet is shown in table 14.

Table 14: Table showing comparison of actual and measured values

Sample Number	Actual Offset (mm)	Offset measured by Software (mm)
Sample 1	25-26	25.146
Sample 2	2-3	2.286
Sample 3	10-11	10.668
Sample 4	18-19	18.542
Sample 5	5-6	5.842

6.6.3 Conclusions: Angled Edges

The offset distance between two corners of the edges can be found out with 100 % accuracy. The least count error can be reduced by decreasing the distance between the camera and the object.

Chapter 7. Future Work and recommendation

7.1 Overview

This chapter gives suggestions regarding the equipments that can be used to enhance the performance of defect detection. This also gives suggestions on how to detect other defects that are not covered in this thesis.

7.2 Equipment

The camera used in the experiments mentioned in this thesis detects both visible and infrared light. As mentioned in the experiments, the light is needed to be placed in a certain position in order to detect the defects. We can use any light, whether it is infrared or visible, but if we are using visible light, then for the light to have an effect on the detection capability of the camera, there should be no interference from light in the environment. In order to avoid environmental interference, an arrangement to block light from the environment has to be made, which can be very costly. To avoid that cost, a camera with visible light filter should be used and infrared lights should be used for defect detection. In this way, the camera will automatically filter out other lights from the environment and will only detect infrared lights.

A lower resolution camera can be used; The camera with this resolution can measure features even less than 1mm, as a result, it detects slight variation in the grain structure of the sheets as a spot which is highly undesirable. By implementing a lower resolution camera accuracy to detect spots will increase.

7.3 Defect detection

The defects that are not covered in this thesis are wrinkles, tear, dents and scratches. These defects occur as a line in the image with a slight difference in color/shade as compared to rest of the image. All these defects can be detected using the software tool called "Count edges." Ideally, there should not be any edges within the sheet, if there is even a single edge present within the sheet, then that can be due to wrinkles, dent, scratch or tear.

7.4 Software Tools

There is one feature that can be added to the software which will make defect detection easier and accurate, i.e. In edge detection tool, there are only four options for contrast value that can be selected; there should be more values so that the least count error is removed.

7.5 Lighting

In the experiments presented in this thesis, only one front light was used, which limited the area in which the spots can be detected and theoretically it will also limit the area in which dent, wrinkles, scratches and a tear can be detected, so more lights should be used to ensure even illumination of the whole sheet.

Number of lights to be used is also dependent on the defect, for example, only one light is needed for chromic aberration; however, for spots, more than one is needed to detect spots at the entire sheet, so the number of lights should be chosen judiciously.

7.6 Inspection station

An inspection station could be set up with multiple numbers of lights and can be programmed to take multiple images under different lighting conditions. Each image can be scanned for some defects depending on the lighting conditions used for capturing that image. A concept drawing of inspection station is given in Figure 42. A sample logic that can be used is given in Figure 43.

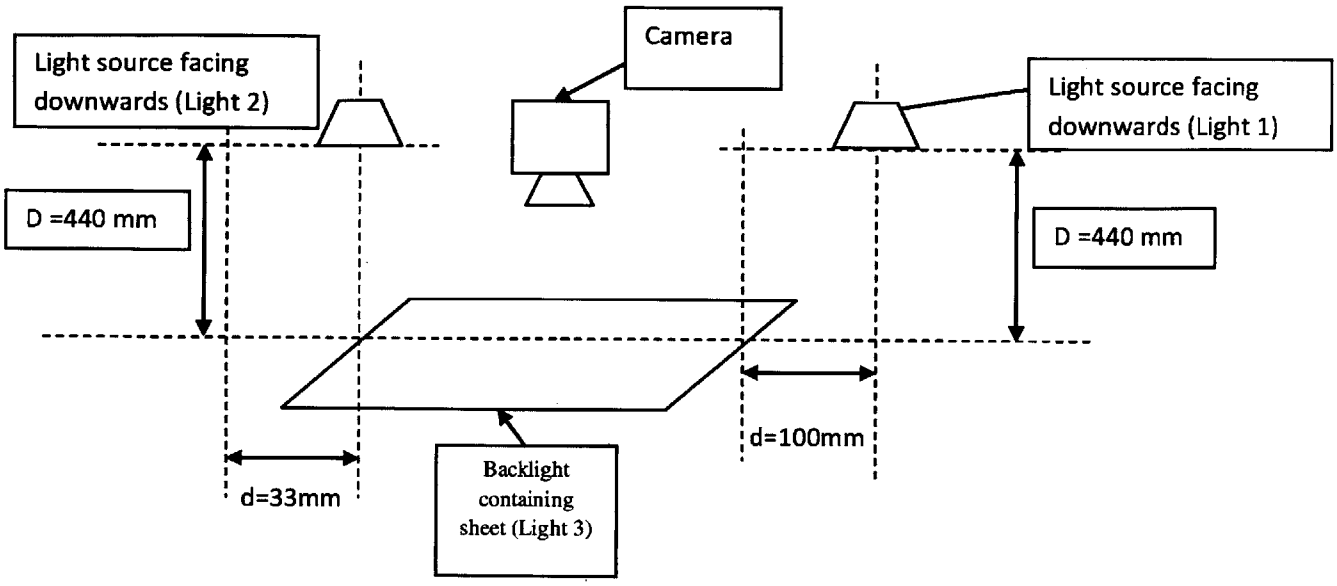

Figure 42: Figure showing a concept drawing of the inspection station.

The heat spreader material can be placed on the surface of backlight using a pick and place robot as described in Chase Olle's thesis [23].

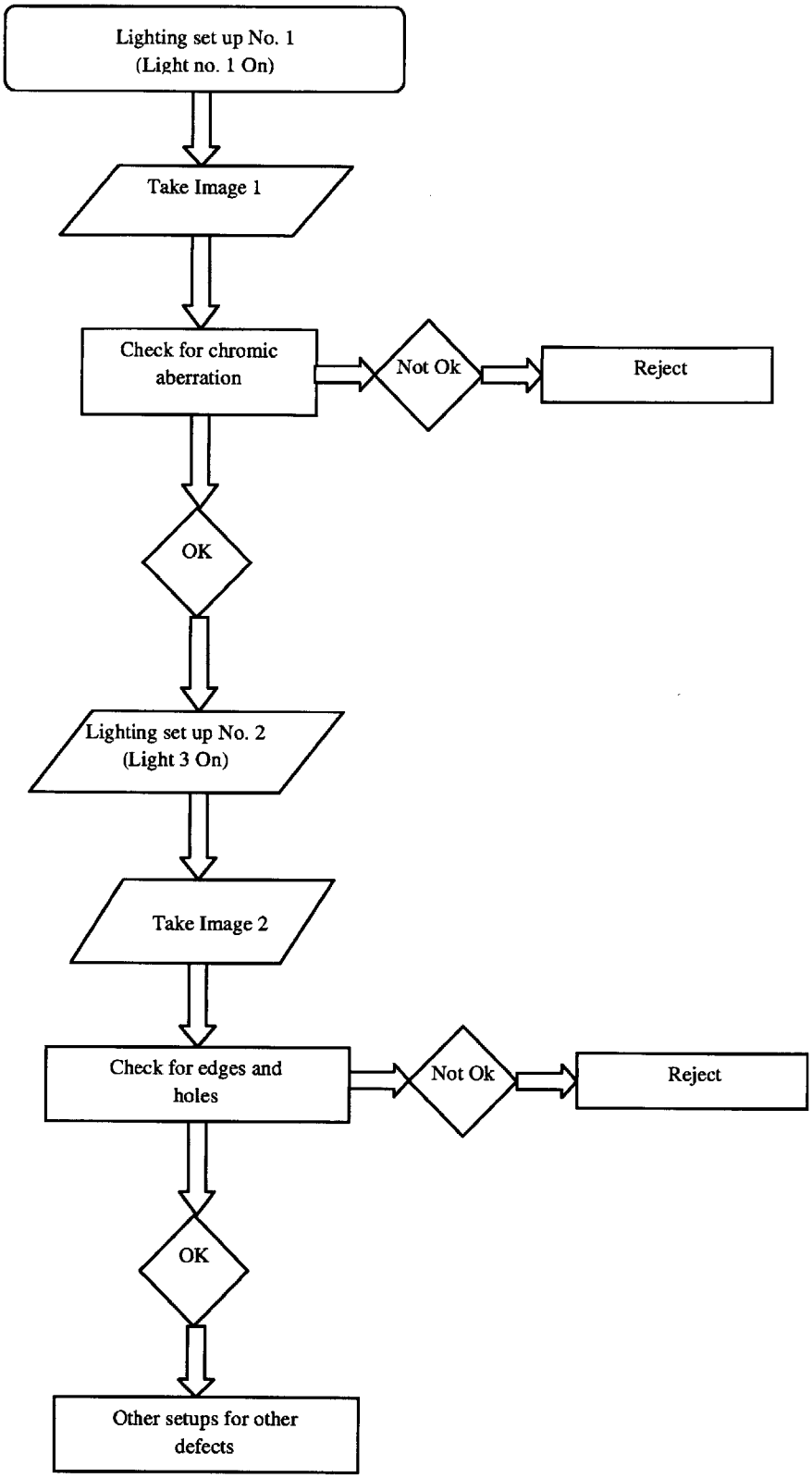

Figure 43: Figure showing sample flow chart of inspection station operations

Chapter 8. Bibliography

[1] Ballard Power Systems Inc. *Ballard Sells U.S. Material Products Division*. 31 Jan. 2013. Last Accessed: April 4, 2014 <http://www.ballard.com/about-ballard/newsroom/news-releases/news01311302.aspx>.

[2] AvCarb Website. Mar. 2014. Accessed: 04 Apr. 2014. <http://www.avcarb.com/>.

[3] Brown, Alan. "Brighter LEDs to Use Metal Matrix Composites." Frost & Sullivan, 20 Feb. 2003. Last Accessed: April 4, 2014

[4] Zhang, G., & Kandlikar, S. G. (2012). A critical review of cooling techniques in proton exchange membrane fuel cell stacks. International Journal of Hydrogen Energy, 37(3), 2412–2429.

[5] Inagaki, M., Ohta, N., & Hishiyama, Y. (2013). Aromatic polyimides as carbon precursors. Carbon, 61, 1–21. doi:10.1016/j.carbon.2013.05.035

[6] M. Inagaki, S. Harada, T. Sato, T. Nakajima, Y. Horino, and K. Morita, "Carbonization of polyimide film 'Kapton,'" Carbon N. Y., vol. 27, no. 2, pp. 253–257, Jan. 1989.

[7] Hishiyama, Y., Igarashi, K., Kanaoka, I., Fujii, H., Kaneda, T., Koidesawa, T. Yoshida, A. (1997). Graphitization behavior of Kapton-derived carbon film related to structure, microtexture and transport properties. *Carbon*, *35*(5), 657–668.

[8] Y. Kaburagi and Y. Hishiyama, "Highly crystallized graphite films prepared by high-temperature heat treatment from carbonized aromatic polyimide films," *Carbon N. Y.*, vol. 33, no. 6, pp. 773–777, Jan. 1995.

[9] "Atomic Resolution Images in Air of Highly Ordered Pyrolytic Graphite (HOPG) Using STM Equipment from NanoSurf." NanoSurf, Jan. 2013. Accessed: April 4, 2014. http://www.azonano.com/article.aspx?ArticleID=1858

[10] Takeichi, T., Eguchi, Y., Kaburagi, Y., Hishiyama, Y., & Inagaki, M. (1998). Carbonization and graphitization of Kapton-type polyimide films prepared from polyamide alkyl ester. *Carbon*, *36*(1-2), 117–122.

[11] Hall, Ernest L. *Computer Image Processing and Recognition*. New York: Academic, 1979. Print.

[12] Gonzalez, Rafael C., and Paul A. Wintz. *Digital Image Processing*. Reading, MA: Addison-Wesley, 1987. Print.

[13] Shapiro, Linda G., and George C. Stockman. *Computer Vision*. Upper Saddle River, NJ: Prentice Hall, 2001. Print.

[14] Baumer Group. *Eyeing Your Quality.* (n.d.): n. pag. Web < http://www.baumer.com/fileadmin/user_upload/international/Downloads/BR-CT/Baumer_VeriSens_BR_EN_1405_11118246.pdf>

[15] "MB-BL10X12." *MetaBright™ High Power Area Backlight 10 X 12 Inch*. N.p., n.d. Web. 30 June 2014.

[16] "ISO-8." *MetaBright™ Exolight™*. N.p., n.d. Web. 30 June 2014.

[17] Rutter, Kathryn. "Defect Identification." E-mail interview. 2 June 2014.

[18] H. Hatori, Y. Yamada, and M. Shiraishi, "In-plane orientation and graphitizability of polyimide films: II. Film thickness dependence," Carbon N. Y., vol. 31, no. 8, pp. 1307–1312, Jan. 1993.

[19] GrafTech International Holdings Inc. (2007). Grafoil Products: The most recognized and most trusted brand of flexible graphite in the world.

[20] "Kapton® MT." DuPont, Dec. 2011. Last Accessed: April 4, 2014. <http://www2.dupont.com/Kapton/en_US/products/MT/>.

[21] "Pyrolytic Graphite Sheet (PGS) Heat Spreading Material" Panasonic, Last Accessed: April 4, 2014. <http://www.panasonic.com/industrial/electronic-components/protection/pyrolytic-graphite-sheet.aspx>.

[22] "Optic Basics - Calculation of the Optics." *Optic Basics*. N.p., n.d. Web. 20 July 2014.

[23] Olle, Chase. "Implementation of Automatic Production Line." Thesis. Massachusetts Institute of Technology, 2014. Print

[24] Svenson, Knute. "The Addition of a Calender Machine to a Pyrolytic Graphite Sheet Production Plant." Thesis. Massachusetts Institute of Technology, 2014. Print

[25] "Exposure (photography)." *Wikipedia*. Wikimedia Foundation, 08 July 2014. Web. 14 Aug. 2014. <http://en.wikipedia.org/wiki/Exposure_%28photography%29>.